

Selected Paper

Functionalized Calix[4]resorcinarene Cavitands. Versatile Platforms for the Modular Construction of Extended Molecular Switches

Vladimir A. Azov, Anna Schlegel, and François Diederich*

Laboratorium für Organische Chemie, Department of Chemistry and Applied Biosciences, ETH Zurich, Hönggerberg, HCI, CH-8093 Zürich, Switzerland

Received April 20, 2006; E-mail: diederich@org.chem.ethz.ch

We report the synthesis and investigation of the vase–kite conformational switching of bridged calix[4]resorcinarene-based cavitands bearing iodo or ethynyl substituents on the upper rim of the cavity. These reactive centers make the cavitands versatile platforms for further modular extension by means of Sonogashira cross-couplings, thereby enabling the construction of diverse functional architectures that are switchable between two highly restricted conformations and that undergo geometrically defined expansions/contractions on the multi-nanometer scale. This is illustrated by attachment of oligo(phenyleneethynyl) fragments, bearing terminal donor and acceptor BODIPY (dipyrromethene boron difluoride) dyes, to a diiodo-substituted cavitand. The multi-nanometer-sized switching motion between the expanded kite and the contracted vase states, induced by temperature or pH changes, was proven by ^{1}H NMR spectroscopy and FRET (fluorescence resonance energy transfer) measurements. The cavitand system, with its modular construction scheme, holds promise to become a general tool for controlled on/off switching of excimer and exciplex formation, PET (photoinduced electron-transfer), or other processes and for investigating the distance dependence of the underlying intermolecular interactions.

The design and preparation of molecular devices capable of large reversible mechanical movements have become a hot area of research in recent years.[1] These structures, mimicking natural phenomena, such as muscle contraction/expansion, bear significant potential for nano-construction, nano-manipulation, design of molecular machines and electron-transfer devices, and information storage. Large motions between bistable states with considerably different geometries, triggered electrochemically or in ionic reactions, have led to remarkable long-range shuffling,[2,3] contraction/expansion,[4] coiling/uncoiling,[5] and shape-flipping in molecular and supramolecular systems.[6–8] On the other hand, the conformational space of the contracted and expanded states in most of the reported systems is quite large, generating substantial uncertainties about the actual geometric orientation of the moving molecular and supramolecular components. This observation led to our interest in the development of large-scale molecular switching systems in which both states adopt precisely defined, rigid geometries.[9]

Quinoxaline-bridged calix[4]resorcinarene cavitand **1** (Fig. 1), introduced by Cram and co-workers,[10] adopts two conformations with profoundly different geometries: a closed vase conformation (C_{4v} symmetry), with a distance of about 0.8 nm between opposite quinoxaline flaps featuring a hydrophobic cavity suitable for guest encapsulation,[11] and an open kite conformation (C_{2v} symmetry) with a flat, extended surface approximately 1.25×1.8 nm in size. Fully reversible switching from the vase to the kite conformation occurs upon variation of temperature[10] or pH,[12] as well as upon metal ion addition.[13] The vase conformer is prevalent at neutral pH at or above room temperature, whereas the kite conformer is predominant at temperatures ≤ 213 K, or upon addition of acid, such as trifluoroacetic acid (TFA), or Zn^{II} ions. The temperature dependence of the vase–kite equilibrium is caused by solvation effects:[10,14] at low temperatures, solvation of the larger, solvent-exposed surface favors the kite conformer whereas at higher temperature, the entropic term $T\Delta S_{solv}$ for solvation of the larger kite surface becomes unfavorable and the vase conformation predominates. The driving force for vase $\rightarrow$ kite switching at low pH presumably is the protonation of the mildly basic quinoxaline N-atoms, which leads to repulsive Coulombic interactions leading to the opening of the vase conformation. The switching process is conveniently monitored by ^{1}H NMR spectroscopy since the chemical shift of the methine H-atoms in the octol bowl is highly conformation-dependent.[10] In the vase conformation, the methine protons appear at $\delta \approx 5.6$ ppm whereas they appear in the kite conformation at about $\delta \approx 3.7$ ppm.

Extension of the wall components[15] increases the distance between their termini in the kite but not in the vase conformation, leading to molecular switching between geometries of increasingly different extensions. In a general modular approach, we chose to prepare cavitands **2** and **3** featuring differently sized, rigid oligo(phenyleneethynyl) arms attached to the two *N*-arylated diazaphthalimide cavity wall flaps in *anti* (**2**) and *syn* (**3**) position (Fig. 2). The rigid attachment of the rod-like arms ensures that the conformational space in the extended kite conformation remains highly restricted and the separation of their termini (R^1 and R^2 in Fig. 2) well defined. This way, it should be possible to switch the interplanar distance of terminal chromophores between ca. 0.8 nm (vase) and ca. $(3.0 + 2r)$ nm (kite, with r the distance between the termini and the arylimide anchor) as illustrated in Fig. 2. Such a modular system promises to become a general tool for controlled

Published on the web December 13, 2006; doi:10.1246/bcsj.79.1926

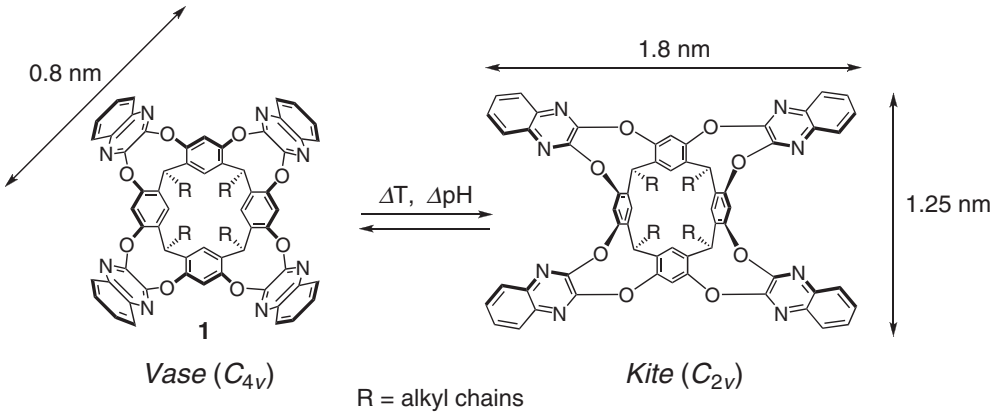

Fig. 1. Vase–kite switching of the quinoxaline-bridged calix[4]resorcinarene cavitand **1**.

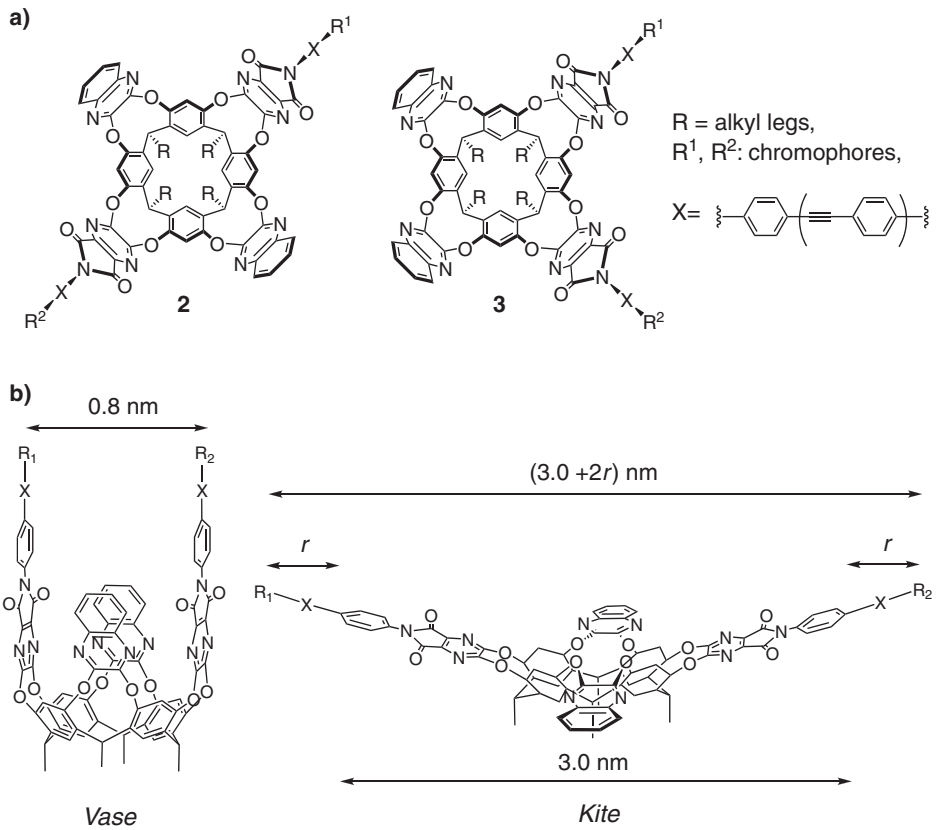

Fig. 2. a) Differentially bridged cavitands bearing oligo(phenyleneethynyl) arms with terminal chromophores R^1 and R^2 in *anti* (**2**) and *syn* (**3**) orientation. b) Distances between terminal chromophores ($R^1 = R^2$) in the vase and kite conformations of anti-substituted cavitand **2**. Legs are omitted for reasons of clarity.

on/off switching of processes, such as excimer and exciplex formation, or photoinduced electron-transfer (PET), and for investigating the distance dependence of the underlying intermolecular interactions. This is illustrated by attachment of terminal donor and acceptor BODIPY (dipyrromethene boron difluoride) dyes leading to fluorescence resonance energy transfer (FRET)[16] that is strongly dependent on the conformational state of the system.[9]

Results and Discussion

Synthesis of Monoethynylated Cavitands. A variety of modifications of the cavity walls in bridged calix[4]resorcinarenes have been reported with different moieties substituting one or two of the quinoxaline rings in the parent cavitand structure **1**.[11c,15,17–19] For the preparation of monoalkynylated cavitand **4**, TMS-protected 4-ethynylaniline **5**[20] was condensed with 5,6-dichloropyrazine-2,3-dicarboxylic anhydride **6** to give imide **7** (Scheme 1). Tris-quinoxaline-cavitand **8**[11c] was subsequently bridged with imide **7** under standard conditions (K_2CO_3/Me_2SO, 20 °C) to yield macrocycle **9** in 62% yield. Unfortunately, all efforts to deprotect the terminal alkyne (*n*-Bu_4NF, CsF, K_2CO_3, or borax ($Na_2B_4O_7 \cdot 10H_2O$) in THF or MeOH/THF) to form cavitand **4** were unsuccessful and only polar decomposition products were detected by thin-layer

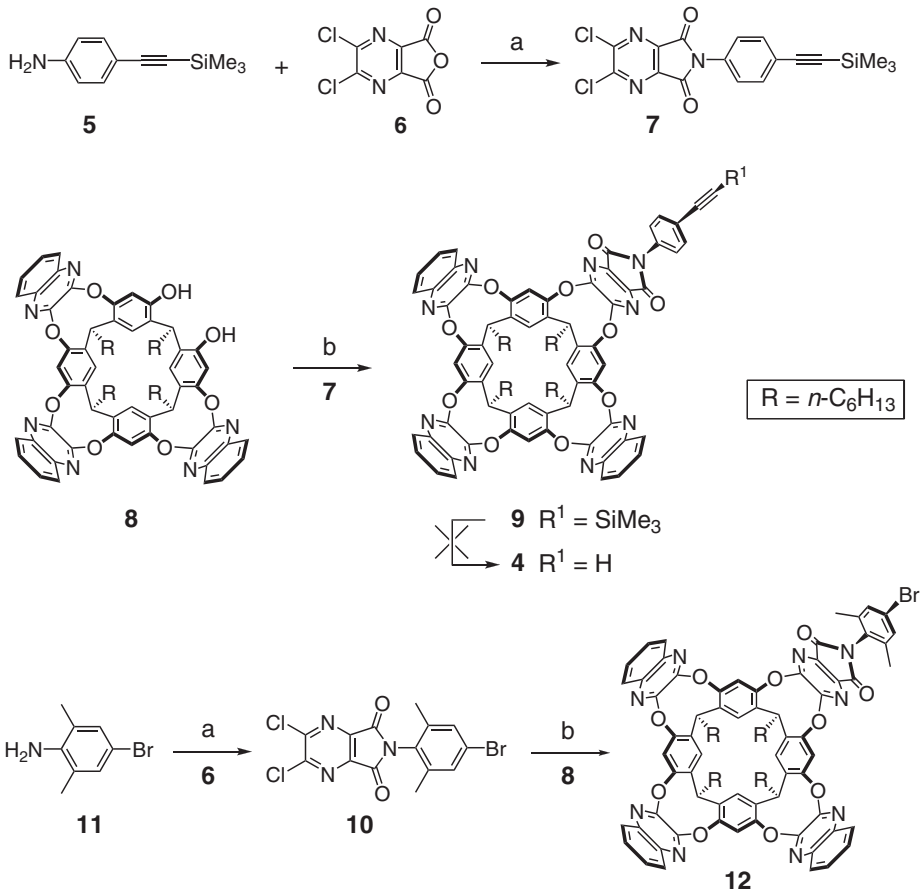

Scheme 1. Synthesis of monofunctionalized cavitands. (a) THF, 30 min, 40 °C; then $(COCl)_2$, Py, 50 °C, 16 h; 71% (**6**), 88% (**10**). (b) K_2CO_3, Me_2SO, 16 h, 62% (**9**), 80% (**12**). THF = tetrahydrofuran, Py = pyridine.

chromatography (TLC). We have previously observed, that this class of cavitands is quite sensitive to nucleophilic attack (F, HO, MeO), leading to cleavage of the ether bridges between the quinoxaline moieties and the octol base scaffold to open the rather strained 9-membered rings. In addition, phthalimides and, even more so the diaza derivatives used in this synthesis, are readily ring-opened in the presence of base under very mild conditions, as we had noted in another report.[21]

To stabilize the labile imide moiety and also to enhance the solubility of these derivatives, we prepared a 5,6-dichloropyrazine-2,3-dicarboximide **10** with methyl substituents *ortho* to the *N*-aryl bond, starting from a commercial aniline **11**. From density functional theory calculations (B3LYP/6-31G*),[22] the torsional angle between the planes of the imide and the *N*-aryl ring would change from ca. 0° in the *N*-phenylated to ca. 70° in the 2,6-dimethylphenylated derivative. In this orientation, the Bürgi–Dunitz approach angle for nucleophilic attack at the imide carbonyls is sterically disfavored.[23]

Bridging diol **8** with dichloroimide **10** provided cavitand **12** in 80% yield. ^{1}H NMR studies showed that cavitand **12** underwent reversible temperature- or pH-triggered vase–kite switching similar to the tetraquinoxaline derivative **1**. On the other hand, Sonogashira cross-coupling[24] of cavitand **12** with 1-ethynyl-4-nitrobenzene did not proceed cleanly; the product mixture contained ca. 40% of inseparable starting material even after prolonged reaction times.

We therefore changed from the bromide to the more reactive iodide or, alternatively, directly introduced a terminal alkyne (Scheme 2). For this purpose, iodide **13** was converted on one hand into iodoimide **14** and, on the other, via compound **15**, into ethynylated imide **16**. Bridging cavitand **8** with the two imides subsequently provided the desired functionalized cavitands **17** and **18** in 74 and 88% yield, respectively.

Synthesis of Dialkynylated Cavitands. The *anti*-di-quinoxaline-bridged[25] and *syn*-di-quinoxaline-bridged[15b] calix[4]-resorcinarenes **19** and **20** were bridged (K_2CO_3/Me_2SO) with dichloroimides **14** and **16** to give the terminally diiodinated (**21** and **23**) and ethynylated (**22** and **24**) cavitands, respectively, which are ideal scaffolds for further attachment of rigid arms, such as oligo(phenyleneethynyl) moieties, by Sonogashira cross-coupling (Scheme 3).

All of the new cavitands undergo the vase–kite switching in both temperature- and pH-triggered modes. Interestingly, they displayed a higher preference for the kite conformation than the parent cavitand **1**.[14a] In variable-temperature (VT) ^{1}H NMR runs, complete conversion of monosubstituted cavitands **17** and **18** into the vase form (all multiplets in the ^{1}H NMR spectrum are resolved) occurred at ca. 310 K in CD_2Cl_2, whereas the equilibration of disubstituted cavitands **21**–**24** was only completed at ca. 330 K in CD_2Cl_2 (sealed tube). All structures switched to the kite form at ca. 210 K; at that temperature, in the NMR spectra no residual vase conformer was observed.

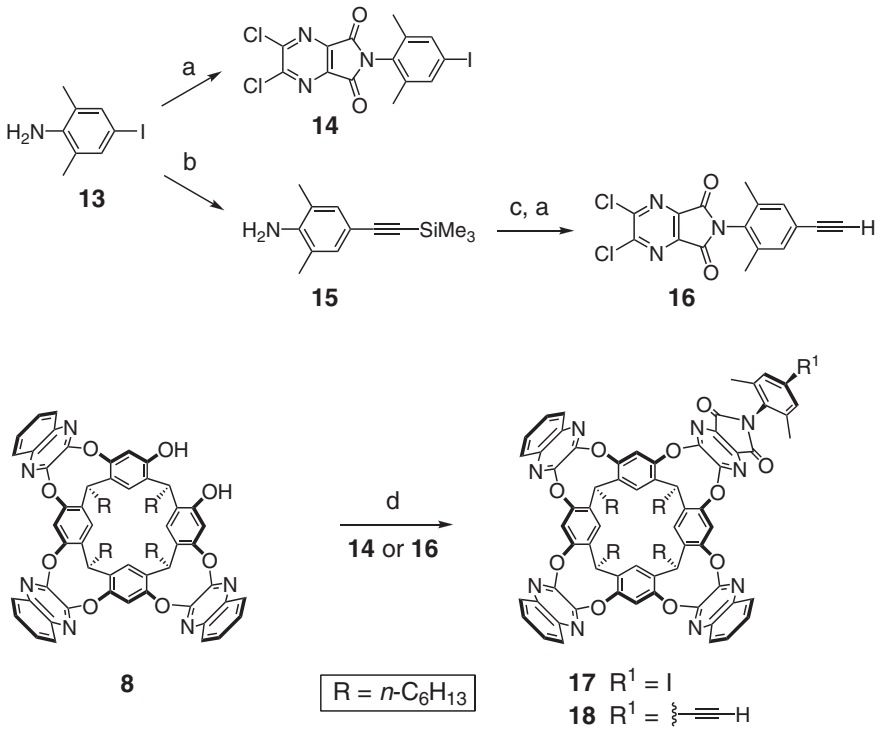

Scheme 2. Synthesis of monofunctionalized cavitands for acetylenic scaffolding. (a) Compound **6**, THF, 30 min, 40 °C; then $(COCl)_2$, Py, 50 °C, 16 h; 91% (**14**), 64% (**16**). (b) $Me_3Si–C{\equiv}CH$, $[Pd(PPh_3)_4]$, CuI, piperidine, 16 h; 100%. (c) NaOH, THF/MeOH 2:1, 3 h; 89%. (d) K_2CO_3, Me_2SO, 16 h; 74% (**17**), 88% (**18**).

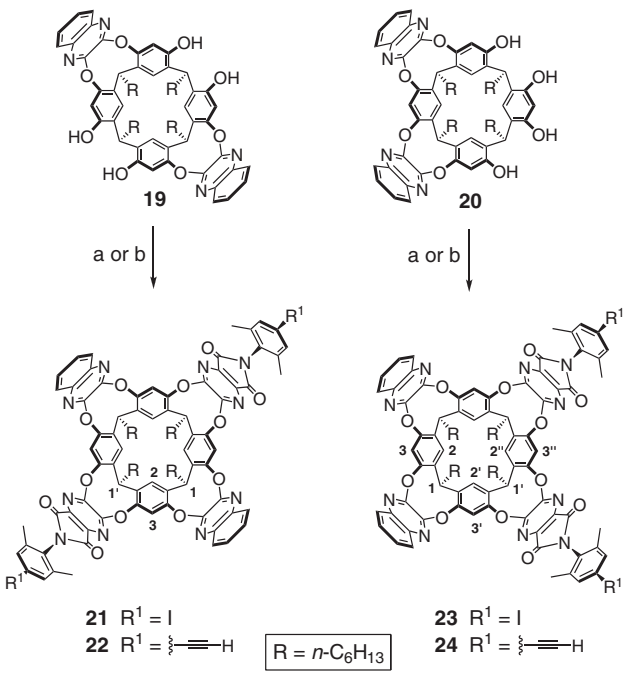

Scheme 3. Synthesis of terminally diiodinated and diethynylated cavitands. (a) Compound **14**, K_2CO_3, Me_2SO, 16–36 h; 38% (**21**), 70% (**23**). (b) Compound **16**, K_2CO_3, Me_2SO, 16–36 h; 55% (**22**), 60% (**24**).

All cavitands completely switched to the kite geometry upon addition of TFA, and this process was reversible upon addition of base (K_2CO_3). A clear trend becomes apparent: the kite geometry becomes more stable upon changing from no wall substitution (**1**), to monosubstituted (**17** and **18**), and to disubstituted (**21**–**24**) cavitands. This trend could arise from two solvation effects acting into the same direction: (i) The kite form becomes increasingly stabilized when a larger surface is favorably solvated. Cram and co-workers explained the preference for the kite geometry at low temperatures with better solvation of the larger surface as compared to the vase surface.[10] (ii) The methyl groups of the 2,6-dimethylphenyl groups attached to the imide moieties sterically prevent favorable solvation of the vase cavity, hence, destabilizing this conformation.[14]

Low-temperature ^{1}H NMR spectra of the *syn*-disubstituted cavitand **24** allowed for the first time the clear observation of the kite1–kite2 equilibration between two non-degenerate structures (Fig. 3). At 203 K, the resonance of the methine protons in the octol base is clearly split, and the signals between 3.4 and 3.8 ppm correspond to four protons in different chemical environments. This splitting is explained by the presence of the two slowly exchanging kite conformations (Fig. 4). At 253 K, the kite1–kite2 conformational equilibration becomes fast, which, together with vase–kite equilibration on the NMR time scale, leads to the disappearance of the methine resonances in the spectrum, due to strong broadening. Finally at 333 K, two resolved triplets around 5.5 ppm are observed for the two sets of methine protons that are in different chemical environments in the vase form. The slow exchange of two kite conformations at 203 K is also visible in the complexity of the aromatic resonances, i.e., the aromatic proton in the octol base, that points towards the hexyl legs, appears in the form of three broad signals around 6.4 ppm. Furthermore at 203 K, two ethynyl resonances appear near 3.2 ppm with the ratio between the two kite conformations of 1:2.3. By means of iterative line-

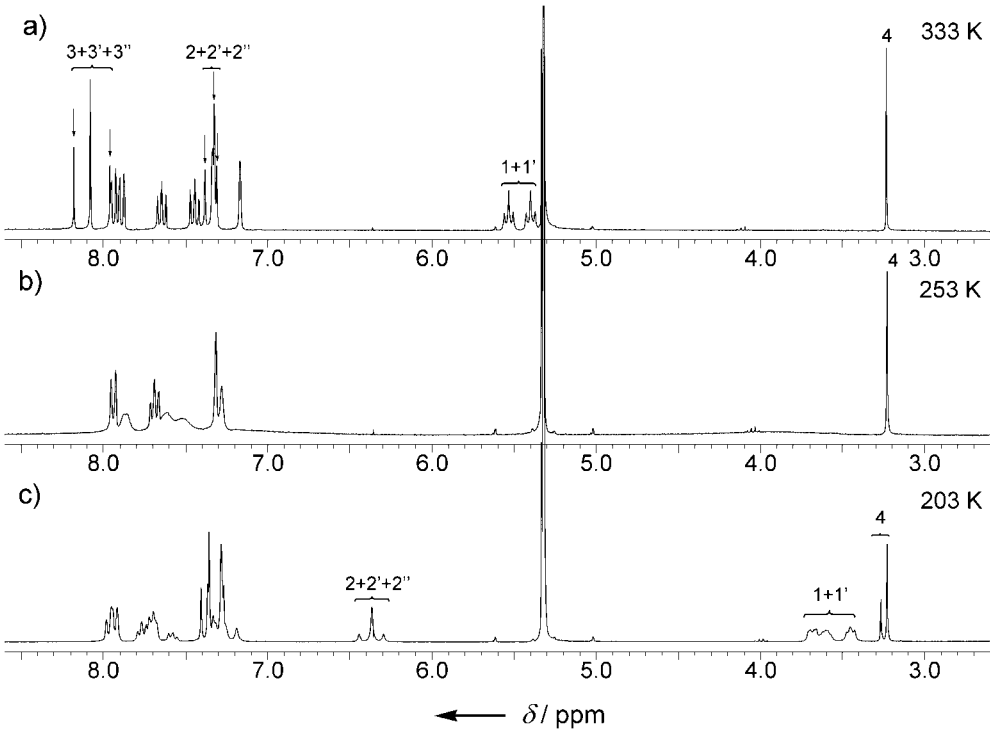

Fig. 3. ^{1}H NMR spectra (CD_2Cl_2, sealed tube) of cavitand **24** at 333 K (a), 253 K (b), and 203 K (c), showing the transition from the vase (a) to two slowly equilibrating, non-degenerate kite conformations. For peak assignments, see Scheme 3. Resonance 4 belongs to the ethyne protons. Resonances at 5.32 ppm belong to residual dichloromethane.

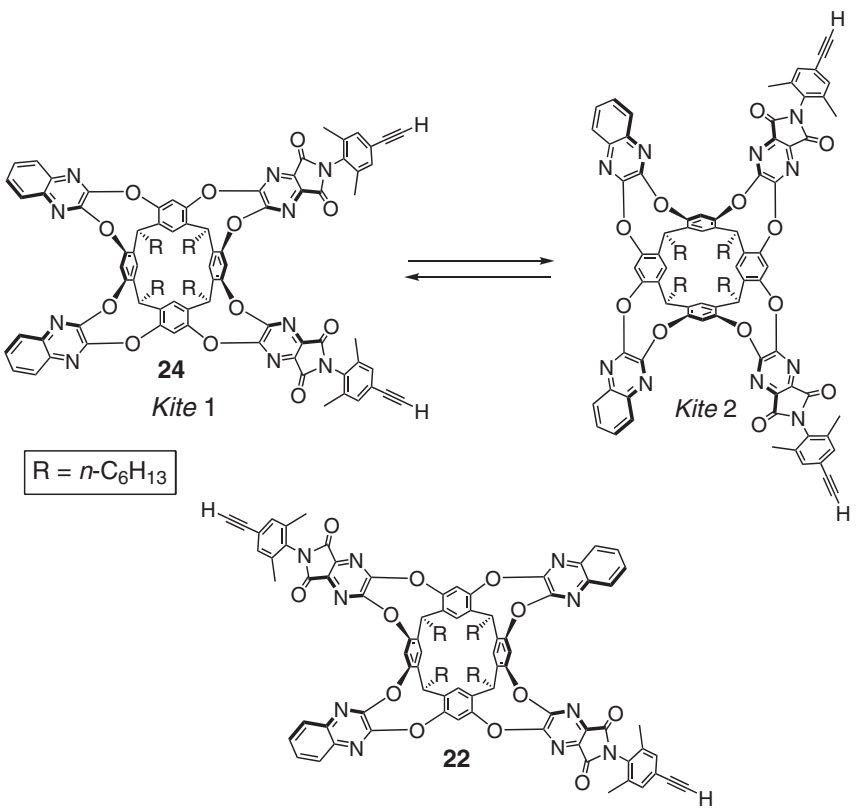

Fig. 4. Conformational switching of cavitand **24** between two non-degenerate kite conformers. As a contrast, the structure of the kite conformer of cavitand **22** is also shown.

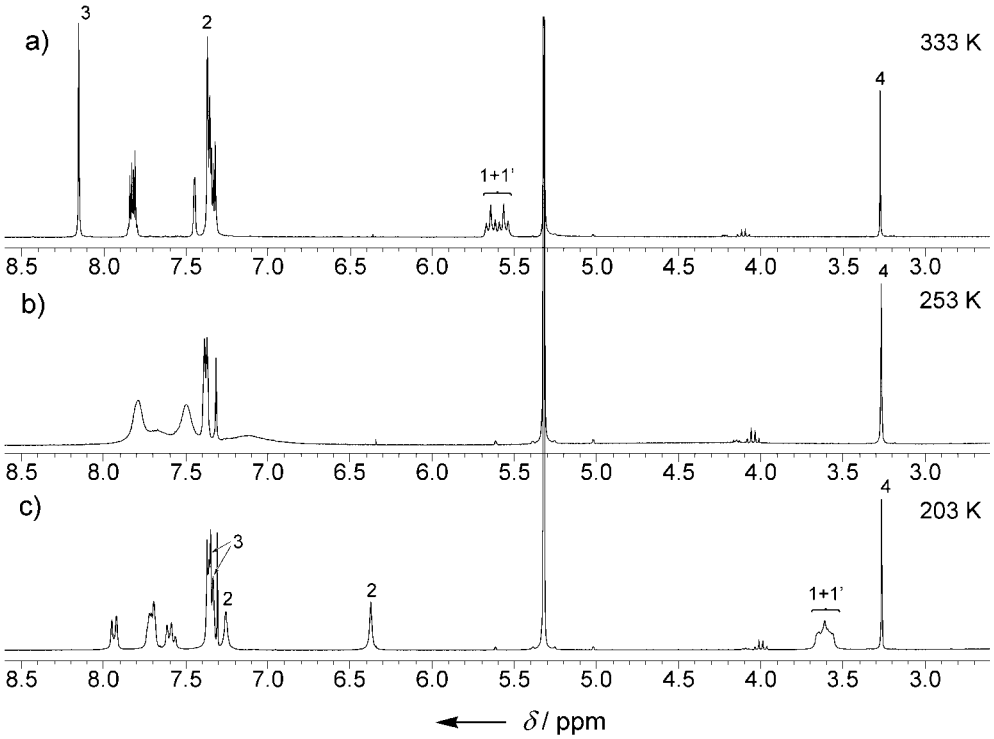

Fig. 5. ^{1}H NMR spectra (CD_2Cl_2, sealed tube) of cavitand **22** at 333 K (a), 253 K (b), and 203 K (c), showing the transition from the vase to two degenerate kite conformations. For peak assignment see Scheme 3. Resonance 4 belongs to ethyne protons. Resonances at 5.32 and 7.26 ppm belong to residual dichloromethane and trichloromethane, respectively.

shape calculations (see the Experimental Section for details), the activation parameters for the kite1–kite2 equilibration of cavitand **24** in CD_2Cl_2 were estimated. The activation enthalpy $\Delta H^{\neq}$ was $62.7 \pm 8\,\mathrm{kJ\,mol^{-1}}$, and the activation entropy $\Delta S^{\neq} = 59.0 \pm 16\,\mathrm{J\,mol^{-1}\,K^{-1}}$. The positive activation entropy is indicative of the release of a significant amount of surface-solvating solvent molecules into the bulk solution in the transition state.

In contrast, kite1–kite2 equilibration of the more symmetric *anti*-diethynylated cavitand **22** leads to two degenerate conformers. Accordingly, the ^{1}H NMR spectrum at 203 K is greatly simplified, particulary, in the aromatic region where the aromatic proton in the octol base on the side of the legs (around 6.4 ppm) appears as one broad singlet (Fig. 5). Also, the splitting pattern of the methine resonances (two different environments) around 3.6 ppm is much less complex.

Synthesis of a Calix[4]resorcinarene Cavitand Undergoing Multi-Nanometer-Sized Expansion/Contraction Motions. As mentioned in the Introduction, cavitands, such as **21**–**24**, provide versatile platforms to attach by cross-coupling, with the help of rigid spacers, different chromophores which in the contracted vase conformation interact at distances of 0.8 nm and below, while being at a multi-nanometer distance in the expanded kite conformation. As a first example for such a giant switching system, we chose the extended structure **25**[9] (Fig. 6) with a donor–acceptor BODIPY (dipyrromethene-boron difluoride) dye pair,[26] attached by rigid oligo(phenyleneethynyl) spacers to the cavitand scaffold, for monitoring the switching dynamics by fluorescence resonance energy transfer (FRET).[16] Molecular models, based on X-ray crystal structure coordinates of bridged calix[4]resorcinarenes in the

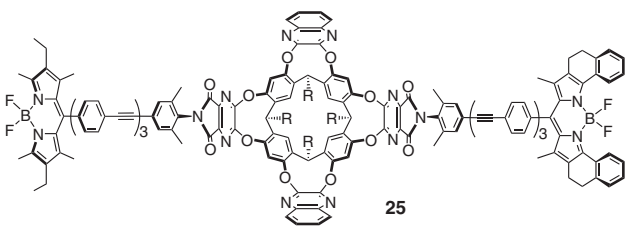

Fig. 6. A giant molecular switch (**25**) with a BODIPY dye pair for monitoring the contraction/expansion motions by FRET techniques.

vase and kite geometry,[13,15b,27] suggested a change in the distance between the two boron atoms of the dye pair from ca. 0.7 nm in the contracted to ca. 7 nm in the expanded state which, according to theoretical considerations, should allow convenient detection of different FRET efficiency in the two states.

The synthesis of cavitand **25** started with the preparation of the dye-appended oligo(phenyleneethynyl)s (Scheme 4). Bright red BODIPY dye **26**,[26b,e] selected as a donor fluorophore for the FRET pair, was efficiently prepared in 60% yield from 2-ethyl-1,3-dimethylpyrrole and 4-iodobenzaldehyde in a 3-step sequence without intermediate purifications. It was subsequently coupled with ethynyl-trimethylsilane to form dye **27**.[26e] Alkyne deprotection of compound **27** demanded optimization since the dye moiety was not stable in the presence of basic *n*-Bu_4NF and other desilylating reagents at room temperature. Finally, it was possible to achieve high yields of compound **28**[26d,e] (longest-wavelength absorption maximum $\lambda_{abs} = 529$ nm, emission maximum $\lambda_{em} = 542$ nm in $CHCl_3$)

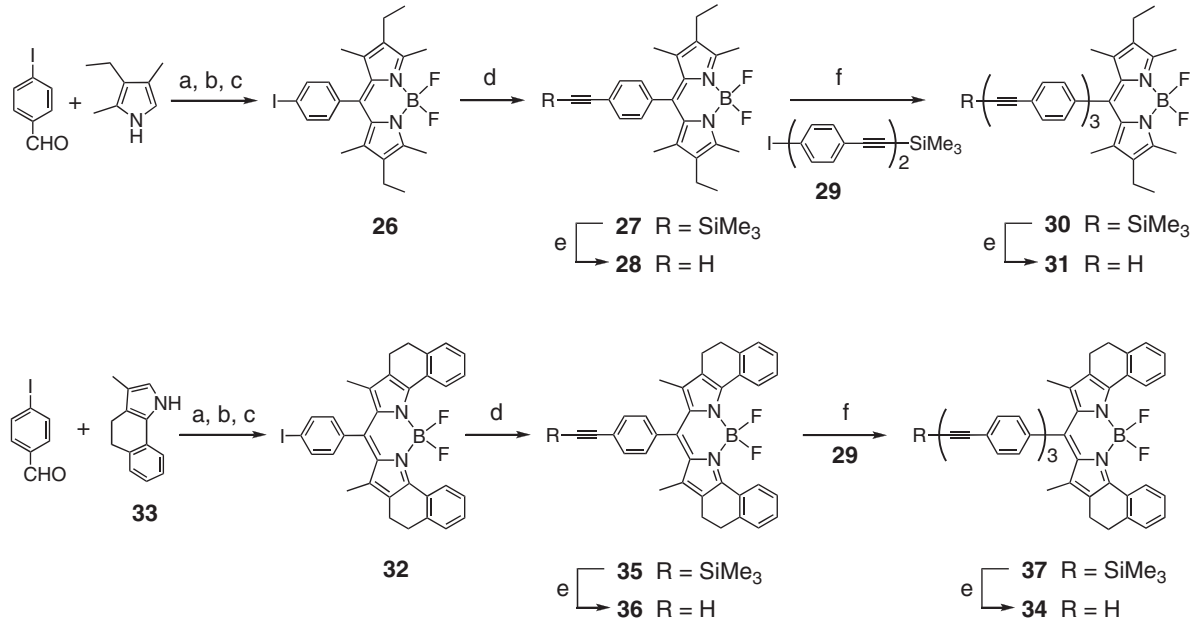

Scheme 4. Synthesis of the BODIPY dye-spacer conjugates **31** and **34**. (a) TFA, CH_2Cl_2, 20 °C, 2–3 h. (b) DDQ, PhMe, 1 h. (c) NEt_3, 20 °C (10 min), then $BF_3 \cdot OEt_2$, 75 °C (30–40 min); 60% (**26**), 75% (**32**) (yields over three steps). (d) $Me_3Si–C{\equiv}CH$, $[Pd(PPh_3)_4]$, CuI, $Et(i\text{-}Pr)_2N$, THF, 20 °C, 1–5 d; 97% (**27**), 99% (**35**). (e) $n\text{-}Bu_4NF$, THF, −78 °C, 30 min; 89% (**28**), 96% (**31**), 98% (**36**), 97% (**34**). (f) $[Pd(PPh_3)_4]$, CuI, $Et(i\text{-}Pr)_2N$, THF, 20 °C, 3–5 d; 74% (**30**), 77% (**37**). TFA = CF_3CO_2H, DDQ = 2,3-dichloro-5,6-dicyano-*p*-benzoquinone.

by deprotecting with $n\text{-}Bu_4NF$ at −70 °C for 30 min and, then, adding 2 equivalents of AcOH to avoid the negative effects of $n\text{-}Bu_4NF$ basicity during workup. Sonogashira cross-coupling of dye **28** with spacer **29**,[20a] followed by alkyne deprotection of compound **30** afforded the desired spacer–donor dye conjugate **31**.

The bronze-red acceptor dye **32**[26c] was obtained in 75% yield in the 3-step sequence starting with the condensation of 3-methyl-4,5-dihydro-1*H*-benzo[*g*]indole **33** with 4-iodobenzaldehyde. A protocol similar to that applied for the preparation of dye derivative **31** afforded the spacer–acceptor dye conjugate **34** via intermediates **35**, **36** ($\lambda_{abs} = 619$ nm, $\lambda_{em} = 630$ nm), and **37**. Compound **34** was only sparingly soluble (ca. 250 μg mL^{-1}) in common organic solvents ($CHCl_3$, PhMe). Nevertheless, it could be purified by using flash chromatography (FC) with large-scale columns, and subsequent Sonogashira cross-couplings could be successfully carried out.

In trial runs, before moving to the final assembly of the giant switch, Sonogashira cross-couplings were performed between mono-functionalized cavitands and donor dyes (**17** and **28**; **18** and **26**; Scheme 5). Both transformations afforded cavitand-dye conjugate **38** in good yields (56 and 64%, respectively) after purification by flash chromatography (SiO_2), followed by gel permeation chromatography (GPC) with Biorad BioBeads SX-1.

The final assembly of switch **25** started with the Sonogashira cross-coupling of cavitand **21** with the donor dye derivative **31** (Scheme 6). The product was first purified by flash chromatography (SiO_2), and the resulting mixture of the mono- and bis-cross-coupled products **39** and **40** was subsequently separated by GPC (CH_2Cl_2). Since the difference in elution time between the two products was very short (only 18

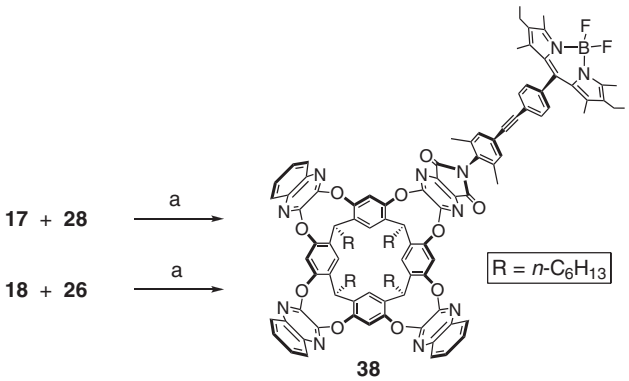

Scheme 5. Synthesis of dye-labeled cavitand **38** (a) $[Pd(PPh_3)_4]$, CuI, $Et(i\text{-}Pr)_2N$, THF, 35 °C, 3 d; 56% (from **17**), 64% (from **18**).

seconds at a retention time of ca. 16 min on an analytical column), several consecutive GPC runs were necessary for complete separation. Cavitands **39** and **40** were obtained in pure form in 28 and 17% yields, respectively (NMR, MS). Both products have good solubility in common nonpolar organic solvents ($CHCl_3$, PhMe).

The second Sonogashira cross-coupling between cavitand **39** and dye derivative **34**, which was monitored by analytical GPC, afforded the target structure **25** with a yield of 49% after flash chromatography and several GPC runs (CH_2Cl_2). The spectral data (NMR, MS, UV–vis, and fluorescence spectroscopy) were in full agreement with the proposed structure and also confirmed the high purity of the cavitand **25**. In the high-resolution matrix-assisted laser-desorption-ionization mass spectrum (HR-MALDI-MS, matrix: 3-hydroxypicolinic

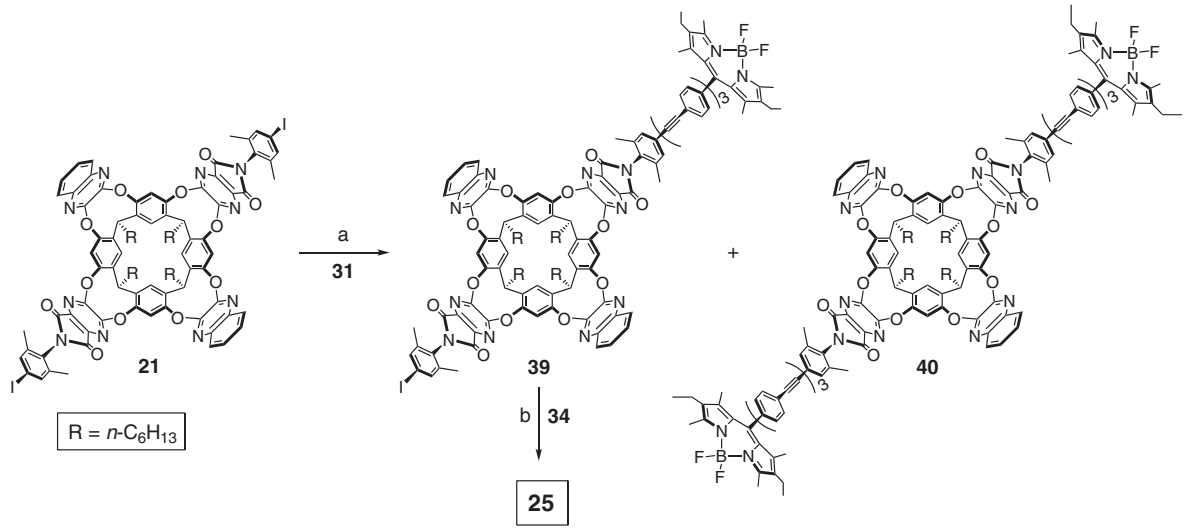

Scheme 6. Synthesis of target compound **25**. (a) Compound **31** (0.75 equiv), [Pd(PPh$_3$)$_4$], CuI, Et(*i*-Pr)$_2$N, THF/CHCl$_3$, 35 °C, 2 d, 28% (**39**), 17% (**40**). (b) Compound **34** (2.25 equiv), [Pd(PPh$_3$)$_4$], CuI, Et(*i*-Pr)$_2$N, THF/CHCl$_3$, 35 °C, 2 d; 49%.

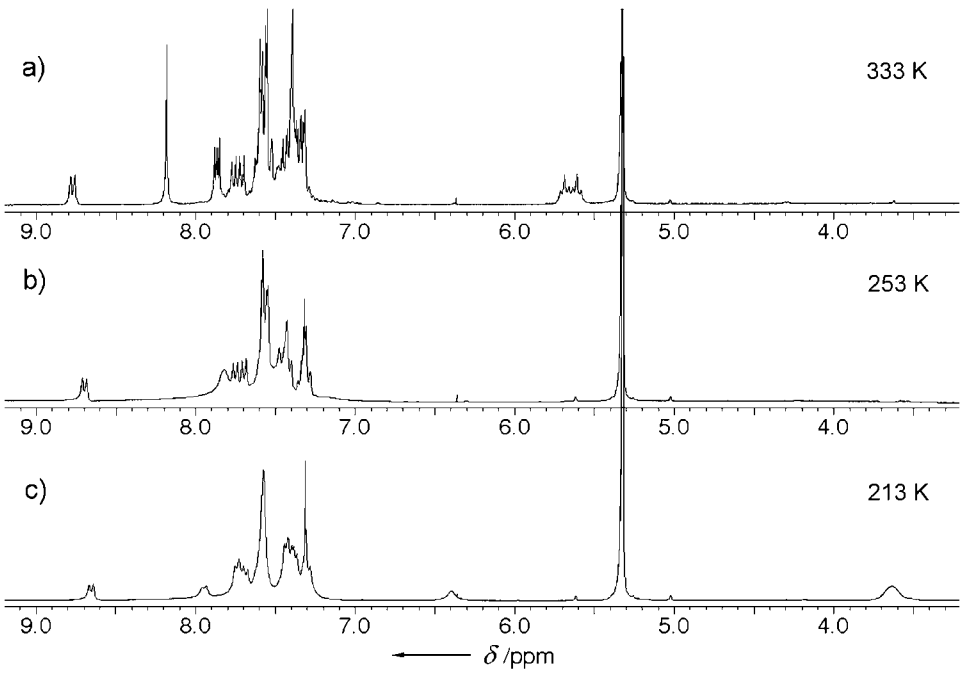

Fig. 7. ^{1}H NMR spectra (CD_2Cl_2, sealed tube) of cavitand **25** at 333 K (a), 253 K (b), and 213 K (c) showing the transition from the vase to the kite conformation.

acid (3-HPA)), the molecular ion after loss of one F atom was observed at m/z 2880.2161 ([$M^+ - F$], $C_{188}H_{156}B_2F_3N_{14}O_{12}^+$; calc. 2880.2160) as the base peak. Despite its large size, target compound **25** displayed good solubility in nonpolar organic solvents ($CHCl_3$, CH_2Cl_2). The reversed sequence of dye addition to cavitand **21** (first compound **34** followed by compound **31**) was inefficient due to the poor solubility of the intermediate mono-dye-labeled cavitand.

Both bis-dye-labeled cavitands **40** and **25** adopt a contracted (vase) conformation (^{1}H NMR spectrum fully resolved) above 293 K in trichloromethane and above 323 K in dichloromethane. Upon lowering the temperature to 213 K or upon addition of TFA (0.3 M), they both undergo expansion to the kite form as clearly evidenced by the characteristic large upfield shift (≈5.6 → ≈3.6 ppm) of the methine protons in the octol scaffold (Fig. 7). The pH-triggered switching was reversible upon addition of base (K_2CO_3). Large-scale expansion/contraction movement of cavitand **25** was also clearly proven by FRET measurements.[9] The UV–vis spectrum in $CHCl_3$ ($c = 1.0 \times 10^{-5}$ M), featuring three strong absorption bands (Fig. 8a) assigned to the oligo(phenyleneethynyl) spacers (λ_{max} 332 nm), the donor dye (529 nm), and the acceptor dye (619 nm), was not affected by the TFA addition ($c = 0.27$ M). Quite opposite, the emission spectrum in $CHCl_3$ ($c = 0.5 \times 10^{-7}$ M, $\lambda_{exc} = 490$ nm, 293 K) changed dramatically upon addition of TFA: the acceptor fluorescence ($\lambda_{em} = 630$ nm) vanished

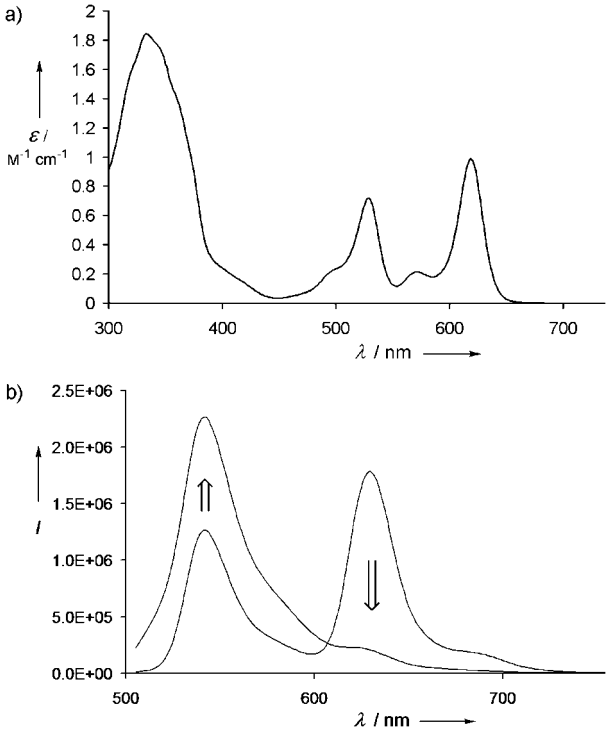

Fig. 8. a) UV–vis spectrum of cavitand **25** in $CHCl_3$ at 20 °C ($c = 1.0 \times 10^{-5}$ M). b) Fluorescence spectra of cavitand **25** in $CHCl_3$ at 20 °C ($c = 0.5 \times 10^{-7}$ M) showing the change after addition of TFA ($c = 0.27$ M).

almost completely, whereas the donor fluorescence ($\lambda_{em} =$ 542 nm) doubled in intensity (Fig. 8b). With a separation of ca. 7 nm between the donor and acceptor dyes in the kite conformation, fluorescence resonance energy transfer is much less efficient than in the vase form with the two dyes in close proximity. This result stays in line with theoretical estimation of the Förster radius R_o for the **26**–**32** donor–acceptor dye pair, which was calculated to be about 4.7 nm for the case of freely rotatong dyes (dye orientation factor $\kappa^2 = 2/3$). We are currently investigating the dynamics of the switching motion of cavitand **25** in single-molecule studies using confocal fluorescence microscopy.[28]

Conclusion

Calix[4]resorcinarene-derived cavitands **17**, **18**, and **21**–**24**, with terminal iodo or ethynyl residues attached to the cavity walls, are versatile platforms for the construction of large-scale molecular switches. Modular extension of these termini by means of Sonogashira cross-couplings enables the construction of functional architectures, which are switchable between two highly restricted conformations and can undergo geometrically defined expansions/contractions on the multi-nanometer scale. This is illustrated by the assembly of the giant molecular switch **25** with terminal donor and acceptor BODIPY dyes, attached by rigid oligo(phenyleneethynyl) spacers to the cavitand platform. The switching motion of cavitand **25** between the expanded kite (ca. 7 nm distance between the two dyes) and the contracted vase state (ca. 7 nm distance), induced by temperature or pH changes, was shown by ^{1}H NMR spectroscopy and FRET measurements. The results of this work pave the way to the design of new dynamic molecular devices and receptors, such as switchable photoinduced energy/electron-transfer systems or molecular grippers for nano-mechanical applications. Furthermore, we believe that these expanded dynamic cavitands can be used as general models for studying the distance dependence of intermolecular interactions such as excimer and exciplex formation both in the bulk as well as at the stage of single molecules. Work in this direction is now underway.

Experimental

General. Melting points were determined using a Büchi Melting Point B-540 and are uncorrected. The melting points of the deeply colored BODIPY derivatives could not be accurately determined. UV–vis spectra were measured on a Varian Cary 500 Scan spectrophotometer in $CHCl_3$ solution. Fluorescence spectra were measured on an Instruments S. A. Fluorolog-3 spectrofluorometer in $CHCl_3$ solution. IR spectra were measured on a Perkin-Elmer Spectrum BX FT-IR spectrometer using neat samples. ^{1}H, ^{13}C, and ^{19}F NMR spectra were recorded with Varian Mercury 300 spectrometers at 300, 75, and 282.5 MHz, respectively. The chemical shifts were recorded relative to $CDCl_3$ (δ 7.26, ^{1}H; δ 77.23, ^{13}C) and CD_2Cl_2 (δ 5.32, ^{1}H; 53.80, δ ^{13}C). C_6F_6 was used as a reference for ^{19}F NMR (δ −161). For the variable temperature experiments, the temperature was calibrated with 100% MeOH ($T \leq 313$ K) or CH_2OH–CH_2OH ($T \geq 313$ K) reference samples. Temperature regulation was stable within ±0.5 K between 363 and 243 K, and within ±1.5 K at lower temperatures. FT-ICR-MALDI-MS were measured on a Ion Spec Ultima FT-ICR-MS (337 nm N_2-laser system) using DHB (2,3-dihydroxybenzoic acid) or DCTB ({(2*E*)-3-[4-(*tert*-butyl)phenyl]-2-methylprop-2-enylidene}malononitrile as a matrix. EI-MS were measured on a VG Analytical Tribrid, U.S.A. Solvents and reagents were purchased reagent-grade and used without further purification. Cavitands **8**,[11c,15b] **19**,[15b,25] **20**,[15b] **25**,[9] **39**,[9] and **40**[9] were prepared according to literature procedures. All reactions were carried out under Ar or N_2. Flash chromatography (FC) was performed using SiO_2 from Fluka or Merck 230–400 mesh (particle size 40–63 μm). Gel permeation chromatography (GPC) was performed using Biorad Bio-Beads SX-1. Anal. thin-layer chromatography (TLC) was performed using precoated SiO_2 glass plates with F-254 fluorescent indicator, and visualization was performed with UV-light at 254 or 366 nm.

General Procedure A for the Preparation of *N*-Arylated Imides of 5,6-Dichloropyrazine-2,3-dicarboxylic Acid. A mixture of aromatic amine (1 molar amount) and compound **6** (1.05 molar amount) in THF under Ar was heated to 40 °C for 30 min. After cooling to 20 °C, $(COCl)_2$ (1.2 molar amount) and pyridine (3 molar amounts) were added. The mixture was stirred for 16 h at 50 °C and, then, filtered through Celite. After evaporation of the solvent, the residue was purified by FC.

General Procedure B for the Bridging of Tris- and Bis-Quinoxaline-Bridged Cavitands 8, 19, and 20. Cavitand and 5,6-dichloropyrazine-2,3-dicarboximide were dissolved in Me_2SO, and the solution degassed by freeze–pump–thaw cycles. K_2CO_3 was added, and the mixture stirred at 35 °C for 16–36 h under Ar. The mixture was diluted with icy H_2O and filtered, and the filtrate washed once more with H_2O and dried over P_2O_5 overnight. The crude product was purified by FC.

General Procedure C for the TMS-Deprotection of Ethynylated Dye Derivatives. The dye derivative (1 molar amount) was

dissolved in THF, ant the solution was cooled to −70 °C. Then, *n*-Bu_4NF (1 M solution, 1.2 molar amount) was added, and the mixture stirred for 30 min. AcOH (2 molar amounts) was added, and the mixture was warmed to 20 °C, filtered through a plug of SiO_2. The solvent was evaporated, and the residue was purified by FC.

2,3-Dichloro-6-[4-(trimethylsilyl)ethynylphenyl]-5*H*-pyrrolo-[3,4-*b*]pyrazine-5,7(6*H*)-dione (7). Compounds **5**[20b] (455 mg, 2.22 mmol) and **6** (510 mg, 2.33 mmol), $(COCl)_2$ (0.238 mL, 2.774 mmol), and pyridine (0.535 mL, 6.66 mmol) were allowed to react in THF (20 mL) according to General Procedure A. Workup and purification by FC (SiO_2; CH_2Cl_2/cyclohexane 4/1) yielded compound **7** (612 mg, 71%) as a light yellow solid. $R_f = 0.4$ (SiO_2; CH_2Cl_2/cyclohexane 4/1); mp 326–327 °C; IR ν 2957, 2897, 1732, 1720, 1546, 1511, 1499, 1393, 1373, 1320, 1224, 1180, 1143, 1125, 1099, 1019, 994, 956, 870, 848, 838, 801, 757, 740, 670, 656, 625 cm^{-1}; ^1H NMR ($CDCl_3$) δ 0.26 (s, 9H), 7.39–7.44 (m, 2H), 7.58–7.63 (m, 2H); ^{13}C NMR ($CDCl_3$) δ 0.09, 96.62, 103.88, 124.34, 126.08, 130.24, 133.08, 143.18, 154.50, 161.09. HRMS Calcd for $C_{17}H_{14}Cl_2N_3O_2Si^+$ ($M^+ + H$): 390.02323. Found (MALDI, matrix: DCTB): 390.023.

(17*s*,18*S*,19*r*,20*R*)-17,18,19,20-Tetrahexyl-15[6]-{4-[(trimethylsilyl)ethynyl]phenyl}-2,4,6,8,10,12,14,16-octaoxa-15[5]*H*-3,7,11-(2,3)-triquinoxalina-15(2,3)-pyrrolo[3,4-*b*]pyrazina-1,5,9,13-(1,2,4,5)-tetrabenzenapentacyclo[11.3.1.1[1,5].1[5,9].1[9,13]]icosaphan-15[5],15[7](15[6]*H*)-dione (9). Compounds **8** (110 mg, 0.092 mmol) and **7** (36 mg, 0.092 mmol), and K_2CO_3 (15 mg, 0.106 mmol) were allowed to react in Me_2SO (2.5 mL) according to General Procedure B for 16 h. Workup and purification by FC (SiO_2; CH_2Cl_2/EtOAc, 1–3%) yielded compound **9** (87 mg, 62%) as a slightly yellowish powder. $R_f = 0.5$ (SiO_2; CH_2Cl_2/EtOAc, 1.2%); mp 325–335 °C (decomp); IR ν 2954, 2926, 2854, 1797, 1738, 1605, 1571, 1481, 1467, 1413, 1397, 1361, 1332, 1247, 1222, 1203, 1149, 1138, 1118, 1081, 1067, 1020, 961, 912, 899, 861, 842, 830 cm^{-1}; ^1H NMR ($CDCl_3$) δ 0.3 (s, 9H), 0.93 (t, $J = 6.4$ Hz, 12H), 1.31–1.49 (m, 32H), 2.24–2.34 (m, 8H), 5.48 (t, $J = 8.1$ Hz, 1H), 5.54–5.62 (m, 3H), 7.09–7.13 (m, 2H), 7.21 (s, 2H), 7.24 (s, 2H), 7.30–7.35 (m, 2H), 7.44–7.50 (m, 2H), 7.51–7.55 (m, 2H), 7.60–7.64 (m, 2H), 7.80–7.84 (m, 4H), 7.92–7.95 (m, 2H), 8.14 (s, 2H), 8.17 (s, 2H); ^{13}C NMR ($CDCl_3$) δ 0.14, 14.28, 22.87, 28.12, 29.58, 32.07, 32.61, 34.52, 96.47, 103.98, 118.67, 119.06, 123.56, 123.77, 123.89, 126.06, 127.65, 127.95, 128.94, 129.25, 129.33, 129.42, 130.77, 132.81, 135.56, 135.72, 135.95, 137.05, 139.68, 139.73, 139.84, 141.14, 152.22, 152.35, 152.43, 152.56, 152.77, 152.80, 153.00, 158.78, 161.35. HRMS Calcd for $C_{93}H_{90}N_9O_{10}Si^+$ ($M^+ + H$): 1520.65799. Found (MALDI, matrix: DCTB): 1520.6555.

2,3-Dichloro-6-(4-bromo-2,6-dimethylphenyl)-5*H*-pyrrolo-[3,4-*b*]pyrazine-5,7(6*H*)-dione (10). Compounds **11** (162.2 mg, 0.811 mmol) and **6** (186.3 mg, 0.851 mmol), $(COCl)_2$ (0.083 mL, 0.973 mmol), and pyridine (0.196 mL, 2.43 mmol) were allowed to react in THF (10 mL) according to General Procedure A. Workup and purification by FC (SiO_2; CH_2Cl_2/cyclohexane 3/1) yielded **10** (285 mg, 88%) as a white solid. $R_f = 0.4$ (SiO_2; CH_2Cl_2/cyclohexane 3/1); mp 279–280 °C; IR ν 1791, 1728, 1575, 1546, 1447, 1384, 1372, 1316, 1259, 1224, 1143, 1114, 1037, 991, 874, 864, 814, 748, 612 cm^{-1}; ^1H NMR ($CDCl_3$) δ 2.12 (s, 6H), 7.37 (s, 2H); ^{13}C NMR ($CDCl_3$) δ 18.18, 124.46, 127.70, 131.96, 138.75, 143.39, 154.56, 161.04.

(17*s*,18*S*,19*r*,20*R*)-15[6]-(4-Bromo-2,6-dimethylphenyl)-17,18,-19,20-tetrahexyl-2,4,6,8,10,12,14,16-octaoxa-15[5]*H*-3,7,11(2,3)-triquinoxalina-15(2,3)-pyrrolo[3,4-*b*]pyrazina-1,5,9,13(1,2,4,5)-tetrabenzenapentacyclo[11.3.1.1[1,5].1[5,9].1[9,13]]icosaphan-15[5],15[7]-(15[6]*H*)-dione (12). Compounds **8** (210 mg, 0.174 mmol) and **10** (69.9 mg, 0.174 mmol), and K_2CO_3 (27.7 mg, 0.201 mmol) were allowed to react in Me_2SO (10 mL) according General Procedure B for 16 h. Workup and purification by FC (SiO_2; CH_2Cl_2/EtOAc, 1%) yielded compound **12** (213 mg, 80%) as a white solid. $R_f = 0.53$ (SiO_2; CH_2Cl_2/EtOAc, 1.2%); mp 380 °C (decomp); IR ν 2926, 2855, 1736, 1578, 1481, 1414, 1399, 1358, 1331, 1259, 1221, 1202, 1158, 1117, 1100, 1065, 912, 897, 857, 839 cm^{-1}; ^1H NMR ($CDCl_3$) δ 0.94 (t, $J = 6.6$ Hz, 12H), 1.05 (s, 3H), 1.32–1.52 (m, 32H), 2.15 (s, 3H), 2.22–2.32 (m, 8H), 5.53–5.69 (m, 4H), 7.21 (s, 2H), 7.24 (s, 2H), 7.30–7.52 (m, 8H), 7.75–7.80 (m, 2H), 7.85–7.91 (m, 4H), 8.19 (s, 2H), 8.22 (s, 2H); ^{13}C NMR ($CDCl_3$) δ 14.29, 17.62, 18.19, 22.88, 28.15, 29.58, 32.09, 32.51, 32.63, 32.76, 34.44, 118.78, 119.33, 123.57, 123.85, 124.15, 127.73, 128.04, 128.13, 128.95, 129.05, 129.14, 129.51, 131.38, 132.06, 135.70, 135.92, 136.00, 137.10, 138.50, 139.31, 139.69, 139.78, 139.93, 141.56, 152.24, 152.54, 152.62, 152.71, 152.87, 153.01, 158.92, 161.42. HRMS Calcd for $C_{90}H_{85}BrN_9O_{10}^+$ ($M^+ + H$): 1530.56028. Found (MALDI, matrix: DCTB): 1530.5613.

2,3-Dichloro-6-(2,6-dimethyl-4-iodophenyl)-5*H*-pyrrolo[3,4-*b*]pyrazine-5,7(6*H*)-dione (14). Compounds **13**[29] (0.741 g, 3.0 mmol) and **6** (0.69 g, 3.151 mmol), $(COCl)_2$ (0.31 mL, 3.6 mmol), and pyridine (1.0 mL, 9.1 mmol) were allowed to react in THF (40 mL) according to General Procedure A. Workup and purification by FC (SiO_2; CH_2Cl_2/cyclohexane 3/1) yielded compound **14** (1.23 g, 91%) as a white solid. $R_f = 0.42$ (SiO_2; CH_2Cl_2/cyclohexane 3/1); mp 312–314 °C; IR ν 1789, 1726, 1703, 1567, 1546, 1470, 1445, 1383, 1373, 1315, 1256, 1235, 1222, 1191, 1142, 1114, 1037, 993, 863, 813 cm^{-1}; ^1H NMR ($CDCl_3$) δ 2.11 (s, 6H), 7.58 (s, 2H); ^{13}C NMR ($CDCl_3$) δ 17.97, 96.80, 128.56, 138.00, 138.75, 143.39, 154.59, 161.01. HRMS Calcd for $C_{14}H_9Cl_2IN_3O_2^+$ ($M^+ + H$): 447.91165. Found (MALDI, matrix: DCTB): 447.9114.

2,6-Dimethyl-4-[(trimethylsilyl)ethynyl]aniline (15). Compound **13**[29] (2.43 g, 9.83 mmol), $[Pd(PPh_3)_4]$ (0.227 g, 0.197 mmol), and CuI (0.028 g, 0.147 mmol) were mixed in piperidine (9 mL), and the mixture degassed by freeze–pump–thaw cycles. Ethynyltrimethylsilane (1.74 mL, 12.3 mmol) was added at 0 °C under Ar, and the mixture was allowed to warm to 20 °C slowly and stirred overnight. The formed precipitate was filtered off, and the solvent evaporated to dryness. FC (SiO_2; CH_2Cl_2/cyclohexane 2/1, then 3/1) yielded compound **15** (2.16 g, 100%) as a slightly brownish liquid. $R_f = 0.3$ (SiO_2; CH_2Cl_2/cyclohexane 2/1); bp 110–120 °C (133 Pa); ^1H NMR ($CDCl_3$) δ 0.23 (s, 9H), 2.13 (s, 6H), 3.72 (br s, 2H), 7.09 (s, 2H); ^{13}C NMR ($CDCl_3$) δ 0.39, 17.54, 91.05, 106.67, 111.86, 121.43, 132.29, 143.68. HRMS Calcd for $C_{13}H_{19}NSi^{++}$ (M^+): 217.12868. Found (EI): 217.1281.

2,3-Dichloro-6-(2,6-dimethyl-4-ethynylphenyl)-5*H*-pyrrolo-[3,4-*b*]pyrazine-5,7(6*H*)-dione (16). Compound **15** (2.16 g, 9.93 mmol) was dissolved in THF/MeOH 2/1 (30 mL), then 1 M NaOH (10 mL) was added. The mixture was stirred for 3 h under Ar and dried with Na_2SO_4, and the solvent evaporated. Purification by FC (SiO_2; CH_2Cl_2/cyclohexane 2/1, then CH_2Cl_2) followed by Kugelrohr distillation in vacuum yielded 2,6-dimethyl-4-ethynylaniline[30] (1.28 g, 89%) as a colorless, readily crystallizing liquid. $R_f = 0.38$ (SiO_2; CH_2Cl_2/cyclohexane 2/1); mp 20–22 °C; bp 120 °C (133 Pa).

2,6-Dimethyl-4-ethynylaniline (400 mg, 2.75 mmol), compound **6** (633 mg, 2.89 mmol), $(COCl)_2$ (0.31 mL, 3.6 mmol), and pyridine (1.0 mL, 9.1 mmol) were allowed to react in THF (30 mL)

according to General Procedure A. Workup and purification by FC (SiO_2; CH_2Cl_2/cyclohexane 3/1) yielded compound **16** (812 mg, 64%) as a white solid. $R_f = 0.6$ (SiO_2; CH_2Cl_2/cyclohexane 2/1); mp 286–287 °C; IR ν 3257, 2924, 1789, 1727, 1597, 1577, 1544, 1475, 1445, 1385, 1374, 1317, 1293, 1237, 1194, 1168, 1142, 1118, 1037, 1009, 993, 892, 883, 838, 814, 749, 730, 718, 678, 632, 613 cm^{-1}; ^1H NMR ($CDCl_3$) δ 2.14 (s, 6H), 3.12 (s, 1H), 7.34 (s, 2H); ^{13}C NMR ($CDCl_3$) δ 18.36, 78.71, 82.73, 124.37, 128.98, 132.46, 136.89, 143.32, 154.41, 160.92. HRMS Calcd for $C_{16}H_9Cl_2N_3O_2^+$ (M^+): 345.00718. Found (EI): 345.0072.

(17*s*,18*S*,19*r*,20*R*)-17,18,19,20-Tetrahexyl-15^6-(4-iodo-2,6-dimethylphenyl)-2,4,6,8,10,12,14,16-octaoxa-15^5*H*-3,7,11(2,3)-triquinoxalina-15(2,3)-pyrrolo[3,4-*b*]pyrazina-1,5,9,13(1,2,4,5)-tetrabenzenapentacyclo[11.3.1.1^{1,5}.1^{5,9}.1^{9,13}]icosaphan-15^5,15^7-(15^6*H*)-dione (17). Compounds **8** (176 mg, 0.146 mmol) and **14** (69 mg, 0.154 mmol), and K_2CO_3 (24 mg, 0.175 mmol) were allowed to react in Me_2SO (10 mL) according to General Procedure B for 16 h. Workup and purification by FC (SiO_2; CH_2Cl_2/EtOAc, 1%) yielded compound **17** (171 mg, 74%) as a white solid. $R_f =$ 0.53 (SiO_2; CH_2Cl_2/EtOAc, 1.2%); mp 330 °C (decomp); IR ν 2925, 2856, 1741, 1569, 1481, 1414, 1399, 1359, 1332, 1255, 1222, 1202, 1159, 1117, 1064, 912, 898, 839, 777, 761, 737, 656, 605 cm^{-1}; ^1H NMR ($CDCl_3$) δ 0.94 (t, $J = 6.6$ Hz, 12H), 1.02 (s, 3H), 1.32–1.52 (m, 32H), 2.13 (s, 3H), 2.22–2.32 (m, 8H), 5.53–5.69 (m, 4H), 7.21 (s, 2H), 7.24 (s, 2H), 7.30–7.36 (m, 2H), 7.44–7.52 (m, 5H), 7.61 (br s, 1H), 7.75–7.80 (m, 2H), 7.85–7.91 (m, 4H), 8.19 (s, 2H), 8.22 (s, 2H); ^{13}C NMR ($CDCl_3$) δ 14.41, 17.49, 18.07, 22.98, 28.25, 29.68, 32.18, 32.60, 32.85, 34.52, 96.46, 118.70, 119.25, 123.49, 123.75, 127.64, 127.96, 128.85, 128.94, 129.05, 129.42, 135.59, 135.81, 135.90, 136.98, 137.26, 137.97, 138.42, 139.21, 139.58, 139.67, 139.82, 141.45, 152.10, 152.40, 152.47, 152.57, 152.73, 152.86, 158.76, 161.23. HRMS Calcd for $C_{90}H_{85}IN_9O_{10}^+$ ($M^+ + H$): 1578.54641. Found (MALDI, matrix: DHB): 1578.5478.

(17*s*,18*S*,19*r*,20*R*)-15^6-(4-Ethynyl-2,6-dimethylphenyl)-17,18,-19,20-tetrahexyl-2,4,6,8,10,12,14,16-octaoxa-15^5*H*-3,7,11(2,3)-triquinoxalina-15(2,3)-pyrrolo[3,4-*b*]pyrazina-1,5,9,13(1,2,4,5)-tetrabenzenapentacyclo[11.3.1.1^{1,5}.1^{5,9}.1^{9,13}]icosaphan-15^5,15^7-(15^6*H*)-dione (18). Compounds **8** (136 mg, 0.113 mmol) and **16** (39 mg, 0.113 mmol), and K_2CO_3 (18 mg, 0.129 mmol) were allowed to react in Me_2SO (5 mL) according to General Procedure B for 16 h. Workup and purification by FC (SiO_2; CH_2Cl_2/EtOAc, 1.5%) yielded compound **18** (147 mg, 88%) as a white solid. $R_f =$ 0.44 (SiO_2; CH_2Cl_2/EtOAc, 1.2%); mp 280–285 °C (decomp); ^1H NMR ($CDCl_3$) δ 0.94 (t, $J = 6.6$ Hz, 12H), 1.04 (s, 3H), 1.32–1.51 (m, 32H), 2.16 (s, 3H), 2.21–2.31 (m, 8H), 3.18 (s, 1H), 5.46–5.67 (m, 4H), 7.21 (s, 2H), 7.24 (s, 2H), 7.29–7.35 (m, 2H), 7.38 (br s, 1H), 7.45–7.52 (m, 5H), 7.75–7.80 (m, 2H), 7.85–7.91 (m, 4H), 8.20 (s, 2H), 8.22 (s, 2H); ^{13}C NMR ($CDCl_3$) δ 14.41, 14.54, 17.80, 18.32, 22.99, 28.24, 29.68, 32.17, 32.60, 32.71, 32.83, 34.54, 78.65, 82.87, 118.69, 119.22, 123.51, 123.77, 124.04, 127.61, 127.94, 128.84, 128.98, 129.07, 129.44, 131.87, 132.59, 135.59, 135.80, 135.87, 136.62, 136.96, 137.42, 139.57, 139.65, 139.81, 141.48, 152.10, 152.37, 152.44, 152.53, 152.73, 152.86, 158.73, 161.31, 171.23. HRMS Calcd for $C_{92}H_{86}N_9O_{10}^+$ ($M^+ + H$): 1476.64977. Found (MALDI, matrix: DCTB): 1476.6500.

(17*s*,18*s*,19*s*,20*s*)-7^6,15^6-Bis(4-iodo-2,6-dimethylphenyl)-17,-18,19,20-tetrahexyl-2,4,6,8,10,12,14,16-octaoxa-7^5*H*,15^5*H*-3,11-(2,3)-diquinoxalina-7,15(2,3)-bis(pyrrolo[3,4-*b*]pyrazina)-1,5,-9,13(1,2,4,5)-tetrabenzenapentacyclo[11.3.1.1^{1,5}.1^{5,9}.1^{9,13}]icosaphan-7^5,7^7(7^6*H*),15^5,15^7(15^6*H*)-tetrone (21). Compounds **19** (189 mg, 0.175 mmol) and **14** (165 mg, 0.368 mmol), and K_2CO_3 (58 mg, 0.42 mmol) were allowed to react in Me_2SO (15 mL) according to General Procedure B for 36 h. Workup and purification by FC (SiO_2; CH_2Cl_2/EtOAc, 1 to 2%) yielded compound **21** (122 mg, 38%) as a white solid. $R_f = 0.38$ (SiO_2; CH_2Cl_2/EtOAc, 1.2%); mp 310–330 °C (decomp); IR ν 2926, 2856, 1797, 1741, 1539, 1481, 1445, 1411, 1358, 1329, 1256, 1234, 1202, 1158, 1116, 1102, 1031, 953, 900, 839, 763, 735, 686 cm^{-1}; ^1H NMR ($CDCl_3$) δ 0.91–0.97 (m, 12H), 1.24–1.56 (m, 32H), 1.36 (s, 6H), 2.17 (s, 6H), 2.22–2.38 (m, 8H), 5.60 (t, $J = 8.1$ Hz, 2H), 5.69 (t, $J = 8.1$ Hz, 2H), 7.26–7.34 (m, 8H), 7.65 (br s, 2H), 7.67 (br s, 2H), 7.83–7.88 (m, 4H), 8.23 (s, 4H); ^{13}C NMR ($CDCl_3$) δ 14.25, 17.78, 17.94, 22.89, 28.14, 29.55, 32.06, 32.28, 32.83, 34.47, 34.56, 96.49, 118.65, 123.89, 128.27, 128.77, 129.44, 135.71, 136.84, 137.39, 137.82, 138.15, 139.16, 139.73, 141.38, 151.96, 152.13, 152.99, 158.71, 161.27. HRMS Calcd for $C_{96}H_{89}I_2N_{10}O_{12}^+$ ($M^+ + H$): 1827.4745. Found (MALDI, matrix: DCTB): 1827.4766.

(17*s*,18*s*,19*s*,20*s*)-7^6,15^6-Bis(4-ethynyl-2,6-dimethylphenyl)-17,18,19,20-tetrahexyl-2,4,6,8,10,12,14,16-octaoxa-7^5*H*,15^5*H*-3,11(2,3)-diquinoxalina-7,15(2,3)-bis(pyrrolo[3,4-*b*]pyrazina)-1,5,9,13(1,2,4,5)-tetrabenzenapentacyclo[11.3.1.1^{1,5}.1^{5,9}.1^{9,13}]-icosaphan-7^5,7^7(7^6*H*),15^5,15^7(15^6*H*)-tetrone (22). Compounds **19** (134 mg, 0.124 mmol) and **16** (90 mg, 0.261 mmol), and K_2CO_3 (40 mg, 0.286 mmol) were allowed to react in Me_2SO (10 mL) according to General Procedure B for 36 h. Workup and purification by FC (SiO_2; CH_2Cl_2/EtOAc, 1.5%) yielded compound **22** (111 mg, 55%) as a white solid. $R_f = 0.52$ (SiO_2; CH_2Cl_2/EtOAc, 1.2%); mp 270–290 °C (decomp); ^1H NMR ($CDCl_3$) δ 0.89–0.95 (m, 12H), 1.31–1.54 (m, 38H), 2.19 (s, 6H), 2.22–2.34 (m, 8H), 3.20 (s, 2H), 5.60 (t, $J = 8.1$ Hz, 2H), 5.69 (t, $J = 8.1$ Hz, 2H), 7.26 (s, 4H), 7.27–7.32 (m, 4H), 7.40 (br s, 2H), 7.42 (br s, 2H), 7.82–7.87 (m, 4H), 8.22 (s, 4H); ^{13}C NMR ($CDCl_3$) δ 14.29, 18.22, 18.26, 22.88, 28.18, 29.58, 32.08, 32.34, 32.88, 34.38, 34.48, 78.92, 82.76, 118.98, 123.95, 124.47, 128.54, 129.46, 129.64, 132.16, 132.98, 135.90, 136.20, 137.05, 137.59, 139.98, 141.64, 152.23, 152.41, 153.28, 159.05, 161.59. HRMS Calcd for $C_{100}H_{91}N_{10}O_{12}^+$ ($M^+ + H$): 1623.68179. Found (MALDI, matrix: DHB): 1623.6793.

(17*R*,18*S*,19*S*,20*R*)-11^6,15^6-Bis(4-iodo-2,6-dimethylphenyl)-17,18,19,20-tetrahexyl-2,4,6,8,10,12,14,16-octaoxa-11^5*H*,15^5*H*-3,7(2,3)-diquinoxalina-11,15(2,3)-bis(pyrrolo[3,4-*b*]pyrazina)-1,5,9,13(1,2,4,5)-tetrabenzenapentacyclo[11.3.1.1^{1,5}.1^{5,9}.1^{9,13}]-icosaphan-11^5,11^7(11^6*H*),15^5,15^7(15^6*H*)-tetrone (23). Compounds **20** (200 mg, 0.186 mmol) and **14** (182 mg, 0.408 mmol), and K_2CO_3 (59 mg, 0.427 mmol) were allowed to react in Me_2SO (10 mL) according to General Procedure B for 16 h. Workup and purification by FC (SiO_2; CH_2Cl_2/EtOAc, 1 to 2%) yielded compound **23** (237 mg, 70%) as a white solid. $R_f = 0.45$ (SiO_2; CH_2Cl_2/EtOAc, 1.2%); mp 255–260 °C (decomp); IR ν 2926, 2856, 1800, 1738, 1540, 1481, 1442, 1412, 1399, 1359, 1331, 1255, 1232, 1199, 1157, 1115, 1100, 1031, 954, 899, 839, 828, 771, 760, 735, 686 cm^{-1}; ^1H NMR ($CDCl_3$) δ 0.93 (t, $J = 6.6$ Hz, 12H), 1.18 (s, 6H), 1.32–1.52 (m, 32H), 2.04 (s, 6H), 2.22–2.32 (m, 8H), 5.45 (br t, $J = 7.5$ Hz, 2H), 5.59 (br t, $J = 7.5$ Hz, 2H), 7.19 (s, 1H), 7.24 (br s, 3H), 7.42–7.61 (m, 8H), 7.87–7.95 (m, 4H), 8.02 (s, 1H), 8.17 (s, 2H), 8.23 (s, 1H); ^{13}C NMR ($CDCl_3$) δ 14.27, 14.41, 17.64, 17.93, 22.86, 28.06, 29.52, 32.01, 32.05, 32.38, 32.54, 34.56, 34.73, 96.32, 118.19, 118.87, 123.71, 123.86, 124.16, 127.73, 128.92, 129.41, 129.76, 135.36, 135.61, 136.50, 137.05, 137.40, 138.03, 138.58, 139.25, 139.78, 141.47, 141.62, 152.36, 152.39, 152.51, 152.88, 153.15, 158.23, 158.31, 160.86, 161.54. HRMS Calcd for $C_{96}H_{89}I_2N_{10}O_{12}^+$ ($M^+ + H$):

1827.47508. Found (MALDI, matrix: DCTB): 1827.4766.

(17*R*,18*S*,19*S*,20*R*)-11^6,15^6-Bis(4-ethynyl-2,6-dimethylphenyl)-17,18,19,20-tetrahexyl-2,4,6,8,10,12,14,16-octaoxa-11^5*H*,15^5*H*-3,7(2,3)-diquinoxalina-11,15(2,3)-bis(pyrrolo[3,4-*b*]pyrazina)-1,5,9,13(1,2,4,5)-tetrabenzenapentacyclo[11.3.1.1^{1,5}.1^{5,9}.1^{9,13}]icosaphan-11^5,11^7(11^6*H*),15^5,15^7(15^6*H*)-tetrone (24). Compounds **20** (80 mg, 0.074 mmol) and **16** (52 mg, 0.149 mmol), and K_2CO_3 (22 mg, 0.159 mmol) were allowed to react in Me_2SO (5 mL) according to General Procedure B for 16 h. Workup and purification by FC (SiO_2; CH_2Cl_2/EtOAc, 1%) yielded compound **24** (72 mg, 60%) as a white solid. $R_f = 0.5$ (SiO_2; CH_2Cl_2/EtOAc, 1.2%); mp 280–290 °C (decomp); IR ν 2924, 2855, 1737, 1576, 1481, 1441, 1413, 1365, 1331, 1263, 1228, 1217, 1201, 1154, 1100, 1064, 1034, 953, 899, 839, 772, 727, 689, 644 cm^{-1}; ^{1}H NMR ($CDCl_3$) δ 0.93 (t, $J = 6.6$ Hz, 12H), 1.24 (s, 6H), 1.32–1.52 (m, 32H), 2.07 (s, 6H), 2.22–2.32 (m, 8H), 3.16 (s, 2H), 5.46 (br t, $J = 7.5$ Hz, 2H), 5.59 (br t, $J = 7.5$ Hz, 2H), 7.19–7.24 (m, 6H), 7.40 (br s, 2H), 7.41–7.61 (m, 4H), 7.88–7.96 (m, 4H), 8.04 (s, 1H), 8.18 (br s, 2H), 8.23 (s, 1H); ^{13}C NMR ($CDCl_3$) δ 14.28, 17.86, 18.17, 22.86, 28.07, 29.53, 32.03, 32.06, 32.39, 32.57, 34.58, 34.74, 78.59, 82.86, 118.19, 118.90, 119.03, 123.70, 123.88, 124.06, 124.15, 127.71, 128.99, 129.44, 129.50, 129.76, 131.96, 132.62, 135.38, 135.62, 136.50, 136.82, 137.05, 137.42, 139.79, 141.51, 141.70, 152.36, 152.41, 152.52, 152.90, 153.18, 158.23, 158.31, 160.93, 161.67. HRMS Calcd for $C_{100}H_{91}N_{10}O_{12}^+$ ($M^+ + H$): 1623.68179. Found (MALDI, matrix: DCTB): 1623.6792.

{3-Ethyl-5-[(4-ethyl-3,5-dimethyl-2*H*-pyrrol-2-ylidene-κN)-(4-iodophenyl)methyl]-2,4-dimethyl-1*H*-pyrrolato-κN}(difluoro)boron (26).[26b,e] 2,4-Dimethyl-3-ethylpyrrole (592 mg, 4.81 mmol) and 4-iodobenzaldehyde (536 mg, 2.31 mmol) were dissolved in CH_2Cl_2 (140 mL) and the solution was degassed by freeze–pump–thaw cycles, then trifluoroacetic acid (0.018 mL, 0.23 mmol) was added. After stirring for 3 h, the mixture was washed with saturated aq $NaHCO_3$ solution, H_2O, and saturated aq NaCl solution, and then dried with Na_2SO_4, and the solvent was evaporated. The solid residue was dissolved in PhMe (70 mL), and a suspension of DDQ (524 mg, 2.31 mmol) in PhMe (70 mL) was added. The mixture was stirred for 1 h at 20 °C, and, then, Et_3N (1.3 mL, 9.2 mmol) was added. After 10 min, $BF_3 \cdot Et_2O$ (2.3 mL, 18.5 mmol) was added, and the mixture heated at 75 °C for 40 min. It was then cooled to 20 °C, and filtered through a plug of SiO_2, and the solvent was evaporated. FC (SiO_2; PhMe/cyclohexane, 2/1) yielded compound **26** (700 mg, 60%) as a dark purple solid. $R_f = 0.43$ (SiO_2; CH_2Cl_2/cyclohexane 1/1); mp 285–290 °C; IR ν 2960, 2925, 2868, 1532, 1471, 1403, 1385, 1370, 1314, 1272, 1259, 1181, 1157, 1113, 1062, 1035, 1009, 971, 865, 827, 751, 730, 698, 656 cm^{-1}; UV–vis λ 529 (ε 77500 M^{-1} cm^{-1}) nm; Fluorescence (λ_{exc} 490 nm) λ_{em} 543 nm; ^{1}H NMR ($CDCl_3$) δ 0.80 (t, $J = 7.5$ Hz, 6H), 1.12 (s, 6H), 2.05 (q, $J = 7.5$ Hz, 4H), 2.56 (s, 6H), 6.24–6.28 (m, 2H), 7.37–7.41 (m, 2H); ^{13}C NMR ($CDCl_3$) δ 11.85, 12.65, 14.73, 17.23, 94.23, 130.32, 130.71, 132.75, 135.60, 137.52, 137.98, 138.82, 154.22; ^{19}F NMR ($CDCl_3$) δ −142.8 (q, $J = 32.5$ Hz). HRMS Calcd for $C_{23}H_{26}BF_2IN_2^+$ (M^+): 506.12018. Found (MALDI, matrix: DHB): 506.1204.

{3-Ethyl-5-[(4-ethyl-3,5-dimethyl-2*H*-pyrrol-2-ylidene-κN)-{4-[(trimethylsilyl)ethynyl]phenyl}methyl]-2,4-dimethyl-1*H*-pyrrolato-κN}(difluoro)boron (27).[26e] Compound **26** (572 mg, 1.13 mmol), [Pd(PPh$_3$)$_4$] (65 mg, 0.057 mmol), and CuI (11 mg, 0.057 mmL) were mixed in dry THF (24 mL), and the mixture was degassed by freeze–pump–thaw cycles. Et(*i*-Pr)$_2$N (1.16 mL, 6.8 mmol) and ethynyltrimethylsilane (0.24 mL, 1.7 mmol) were added, and the bright red mixture was stirred under Ar overnight. The mixture was filtered through Celite and the solvent was evaporated. FC (SiO_2; CH_2Cl_2/cyclohexane 1/1) gave compound **27** (524 mg, 97%) as a bright red solid. $R_f = 0.46$ (SiO_2; CH_2Cl_2/cyclohexane 1/1); mp 244–246 °C; IR ν 2961, 2932, 2872, 2166, 1535, 1475, 1404, 1383, 1360, 1314, 1271, 1260, 1249, 1184, 1158, 1114, 1091, 1050, 974, 864, 840, 760, 709, 654 cm^{-1}; UV–vis λ 529 (ε 75300 M^{-1} cm^{-1}) nm; Fluorescence (λ_{exc} 490 nm) λ_{em} 543 nm; ^{1}H NMR ($CDCl_3$) δ 0.29 (s, 9H), 0.98 (t, $J = 7.8$ Hz, 6H), 1.30 (s, 6H), 2.30 (q, $J = 7.8$ Hz, 4H), 2.53 (s, 6H), 7.22–7.26 (m, 2H), 7.58–7.62 (m, 2H); ^{13}C NMR ($CDCl_3$) δ 0.26, 12.21, 12.84, 14.92, 17.37, 95.74, 104.49, 123.76, 128.47, 130.58, 132.71, 132.99, 136.15, 138.27, 139.26, 154.04; ^{19}F NMR ($CDCl_3$) δ −145.2 (q, $J = 32.5$ Hz). HRMS Calcd for $C_{28}H_{35}BF_2N_2Si^+$ (M^+): 476.26306. Found (MALDI, matrix: DHB): 476.2613.

{3-Ethyl-5-[(4-ethyl-3,5-dimethyl-2*H*-pyrrol-2-ylidene-κN)-(4-ethynylphenyl)methyl]-2,4-dimethyl-1*H*-pyrrolato-κN}(difluoro)boron (28).[26d,e] Compound **27** (455 mg, 0.95 mmol), *n*-Bu$_4$NF (1.15 mL, 1.15 mmol), and AcOH (0.12 mL) were allowed to react in THF (12.5 mL) according to General Procedure C. Workup and purification by FC (SiO_2; CH_2Cl_2/cyclohexane 1/1) afforded compound **28** (345 mg, 89%) as a bright red solid. $R_f = 0.43$ (SiO_2; CH_2Cl_2/cyclohexane 1/1); mp 248–250 °C; IR ν 3265, 2962, 2925, 2870, 1532, 1475, 1403, 1385, 1371, 1314, 1273, 1260, 1183, 1158, 1115, 1072, 1035, 974, 867, 842, 762, 705, 657 cm^{-1}; UV–vis λ 529 (ε 74400 M^{-1} cm^{-1}) nm; Fluorescence (λ_{exc} 490 nm) λ_{em} 543 nm; ^{1}H NMR ($CDCl_3$) δ 0.98 (t, $J = 7.5$ Hz, 6H), 1.30 (s, 6H), 2.30 (q, $J = 7.5$ Hz, 4H), 2.53 (s, 6H), 3.18 (s, 1H), 7.25–7.29 (m, 2H), 7.60–7.64 (m, 2H); ^{13}C NMR ($CDCl_3$) δ 12.20, 12.86, 14.93, 17.38, 83.21, 122.78, 128.61, 130.57, 132.86, 133.06, 136.54, 138.27, 139.08, 154.138; ^{19}F NMR ($CDCl_3$) δ −145.2 (q, $J = 32.5$ Hz). HRMS Calcd for $C_{25}H_{27}BF_2N_2^+$ (M^+): 404.22353. Found (MALDI, matrix: DHB): 404.2224.

{3-Ethyl-5-[(4-ethyl-3,5-dimethyl-2*H*-pyrrol-2-ylidene-κN)-(4-{[4-({4-[(trimethylsilyl)ethynyl]phenyl}ethynyl)phenyl]ethynyl}phenyl)methyl]-2,4-dimethyl-1*H*-pyrrolato-κN}(difluoro)boron (30). Compounds **28** (238 mg, 0.59 mmol) and **29**[20a] (243 mg, 0.606 mol), [Pd(PPh$_3$)$_4$] (27 mg, 0.024 mmol), and CuI (4.5 mg, 0.024 mmL) were mixed in dry THF (24 mL), and the mixture was degassed by freeze–pump–thaw cycles. Et(*i*-Pr)$_2$N (0.60 mL, 3.53 mmol) was added, and the bright red mixture was stirred under Ar for 3 d. The mixture was filtered through Celite, and the solvent was evaporated. FC (SiO_2; CH_2Cl_2/cyclohexane 1/1) gave compound **30** (304 mg, 74%) as a bright red solid. $R_f = 0.49$ (SiO_2; CH_2Cl_2/cyclohexane 1/1); mp 270–275 °C (decomp); IR ν 2959, 2920, 2863, 2155, 1534, 1474, 1405, 1372, 1319, 1264, 1249, 1189, 1160, 1115, 1069, 1051, 978, 862, 838, 760, 708, 649 cm^{-1}; UV–vis λ 336 (ε 70700 M^{-1} cm^{-1}), 529 (ε 74200 M^{-1} cm^{-1}) nm; Fluorescence (λ_{exc} 490 nm) λ_{em} 544 nm; ^{1}H NMR ($CDCl_3$) δ 0.27 (s, 9H), 0.99 (t, $J = 7.5$ Hz, 6H), 1.34 (s, 6H), 2.31 (q, $J = 7.5$ Hz, 4H), 2.54 (s, 6H), 7.29–7.32 (m, 2H), 7.46 (s, 4H), 7.50–7.57 (m, 4H), 7.65–7.68 (m, 2H); ^{13}C NMR ($CDCl_3$) δ 0.27, 12.23, 12.87, 14.95, 17.40, 90.46, 90.90, 91.05, 91.30, 96.70, 104.69, 122.98, 123.08, 123.30, 123.70, 128.68, 130.63, 131.52, 131.72, 132.04, 132.34, 133.05, 136.16, 138.28, 139.24, 154.11; ^{19}F NMR ($CDCl_3$) δ −145.2 (q, $J = 32.5$ Hz). HRMS Calcd for $C_{44}H_{43}BF_2N_2Si^+$ (M^+): 676.32566. Found (MALDI, matrix: DHB): 676.3251.

(3-Ethyl-5-{(4-ethyl-3,5-dimethyl-2*H*-pyrrol-2-ylidene-κN)-

[4-({4-[(4-ethynylphenyl)ethynyl]phenyl}ethynyl)phenyl]methyl}-2,4-dimethyl-1*H*-pyrrolato-*κN*)(difluoro)boron (31). Compound **30** (270 mg, 0.40 mmol), *n*-Bu_4NF (0.48 mL, 0.48 mmol), and AcOH (0.05 mL) were allowed to react in THF (8 mL) according to General Procedure C. Workup and purification by FC (SiO_2; CH_2Cl_2/cyclohexane 1/1) afforded compound **31** (232 mg, 96%) as a bright red solid. $R_f = 0.45$ (SiO_2; CH_2Cl_2/cyclohexane 1/1); mp > 300 °C (decomp); IR ν 3259, 2959, 2925, 2863, 1534, 1473, 1405, 1372, 1312, 1264, 1188, 1159, 1114, 1061, 1041, 975, 834, 760, 703 cm^{-1}; UV–vis λ 334 (ε 68100 M^{-1} cm^{-1}), 529 (ε 76000 M^{-1} cm^{-1}) nm; Fluorescence (λ_{exc} 490 nm) λ_{em} 544 nm; ^1H NMR ($CDCl_3$) δ 0.99 (t, $J = 7.5$ Hz, 6H), 1.34 (s, 6H), 2.31 (q, $J = 7.5$ Hz, 4H), 2.54 (s, 6H), 3.19 (s, 1H), 7.29–7.32 (m, 2H), 7.49 (s, 4H), 7.51–7.57 (m, 4H), 7.65–7.68 (m, 2H); ^{13}C NMR ($CDCl_3$) δ 12.10, 12.74, 14.82, 17.28, 79.35, 83.40, 90.46, 90.96, 91.11, 91.15, 122.38, 123.15, 123.32, 123.64, 123.79, 128.81, 130.74, 131.71, 131.83, 131.86, 132.33, 132.46, 133.17, 136.31, 138.41, 139.37, 154.28. ^{19}F NMR ($CDCl_3$) δ −145.2 (q, $J = 32.5$ Hz). HRMS Calcd for $C_{41}H_{35}BF_2N_2^+$ (M^+): 604.28613. Found (MALDI, matrix: DHB): 676.2864.

Difluoro{2-[(4-iodophenyl)(3-methyl-4,5-dihydro-2*H*-benzo[*g*]indol-2-ylidene-*κN*)methyl]-3-methyl-4,5-dihydro-1*H*-benzo[*g*]indolato-*κN*}boron (32).[26c] Compound **33**[26c] (182 mg, 1.0 mmol) and 4-iodobenzaldehyde (0.112 mg, 0.48 mmol) were dissolved in CH_2Cl_2 (35 mL) and degassed by freeze–pump–thaw cycles, then trifluoroacetic acid (0.004 mL, 0.048 mmol) was added. After stirring for 2 h, the mixture was washed with saturated aq $NaHCO_3$ solution, H_2O, and saturated aq NaCl solution, and then dried with Na_2SO_4. After the solvent was evaporated, the solid residue was dissolved in PhMe (20 mL), and a suspension of DDQ (0.113 mg, 0.48 mmol) in PhMe (20 mL) was added. The mixture was stirred for 30 min at 20 °C, then Et_3N (0.28 mL, 2.0 mmol) was added. After 10 min, $BF_3 \cdot Et_2O$ (0.50 mL, 4.0 mmol) was added, and the mixture heated at 75 °C for 30 min. It was then cooled to 20 °C, and filtered through a plug of SiO_2, and the solvent was evaporated. FC (SiO_2; PhMe/cyclohexane, gradient 30 → 0%) yielded compound **32** (226 mg, 75%) as a dark copper-red solid. $R_f = 0.49$ (SiO_2; CH_2Cl_2/cyclohexane 1/1); mp 310–315 °C (decomp); IR ν 2927, 1550, 1523, 1466, 1432, 1398, 1387, 1367, 1327, 1274, 1230, 1191, 1157, 1113, 1082, 1056, 1048, 1032, 1017, 1007, 962, 944, 911, 870, 820, 767, 750, 730, 719, 708, 699, 678, 625, 616 cm^{-1}; UV–vis λ 619 (ε 127000 M^{-1} cm^{-1}) nm; Fluorescence (λ_{exc} 590 nm) λ_{em} 630 nm; ^1H NMR ($CDCl_3$) δ 1.39 (s, 6H), 2.54 (br t, $J = 7$ Hz, 4H), 2.88 (br t, $J = 7$ Hz, 4H), 7.23–7.44 (m, 8H), 7.87–7.90 (m, 2H), 8.79 (br d, $J = 7.8$ Hz, 2H); ^{13}C NMR ($CDCl_3$) δ 12.75, 20.77, 30.80, 127.46, 128.20, 128.42, 128.75, 129.61, 130.84, 132.31, 133.80, 135.91, 138.44, 140.79, 151.03; ^{19}F NMR ($CDCl_3$) δ −134.5 (q, $J = 34$ Hz).

Difluoro{3-methyl-2-[(3-methyl-4,5-dihydro-2*H*-benzo[*g*]indol-2-ylidene-*κN*){4-[(trimethylsilyl)ethynyl]phenyl}methyl]-4,5-dihydro-1*H*-benzo[*g*]indolato-*κN*}boron (35). Compound **32** (196 mg, 0.313 mmol), [$Pd(PPh_3)_4$] (18 mg, 0.016 mmol), and CuI (3 mg, 0.016 mmL) were mixed in dry THF (10 mL), and the mixture was degassed by freeze–pump–thaw cycles. $Et(i\text{-}Pr)_2N$ (0.32 mL, 1.88 mmol) and ethynyltrimethylsilane (0.088 mL, 0.63 mmol) were added, and the dark green mixture was stirred under Ar for 5 d. The mixture was filtered through Celite, and the solvent was evaporated. FC (SiO_2; CH_2Cl_2/cyclohexane 1/1) gave compound **35** (185 mg, 99%) as a dark copper-red solid. $R_f = 0.42$ (SiO_2; CH_2Cl_2/cyclohexane 3/2); mp 255–270 °C (decomp); IR ν 2934, 2889, 2832, 2154, 1552, 1524, 1466, 1434, 1400, 1386, 1366, 1326, 1305, 1275, 1248, 1229, 1190, 1157, 1082, 1048, 1016, 963, 860, 839, 824, 772, 753, 731, 708, 640 cm^{-1}; UV–vis λ 618 (ε 116000 M^{-1} cm^{-1}) nm; Fluorescence (λ_{exc} 590 nm) λ_{em} 629 nm; ^1H NMR ($CDCl_3$) δ 0.31 (s, 9H), 1.37 (s, 6H), 2.53 (br t, $J = 7$ Hz, 4H), 2.88 (br t, $J = 7$ Hz, 4H), 7.23–7.45 (m, 8H), 7.63–7.69 (m, 2H), 8.80 (br d, $J = 7.8$ Hz, 2H); ^{13}C NMR ($CDCl_3$) δ 0.29, 12.69, 20.76, 30.80, 96.01, 104.48, 124.02, 127.44, 128.18, 128.46, 128.73 (t, $J = 11$ Hz), 128.95, 129.55, 132.22, 132.82, 133.79, 135.99, 136.51, 138.89, 140.76, 150.94; ^{19}F NMR ($CDCl_3$) δ −134.5 (q, $J = 34$ Hz). HRMS Calcd for $C_{38}H_{35}BF_2N_2Si^+$ (M^+): 596.26306. Found (MALDI, matrix: DCTB): 596.2619.

Difluoro{3-methyl-2-[(3-methyl-4,5-dihydro-2*H*-benzo[*g*]indol-2-ylidene-*κN*){4-[(trimethylsilyl)ethynyl]phenyl}methyl]-4,5-dihydro-1*H*-benzo[*g*]indolato-*κN*}boron (36). Compound **35** (143 mg, 0.24 mmol), *n*-Bu_4NF (0.29 mL, 0.29 mmol), and AcOH (0.036 mL) were allowed to react in THF (5 mL) according to General Procedure C. Workup and purification by FC (SiO_2; CH_2Cl_2/cyclohexane gradient 50 → 40%) afforded compound **36** (124 mg, 98%) as a dark copper-red solid. $R_f = 0.33$ (SiO_2; CH_2Cl_2/cyclohexane 3/2); mp 280–300 °C (decomp); IR ν 3288, 2931, 2832, 1553, 1519, 1464, 1431, 1398, 1386, 1366, 1341, 1325, 1309, 1275, 1229, 1191, 1155, 1082, 1045, 1016, 962, 945, 842, 822, 771, 751, 727, 713, 667, 643, 617 cm^{-1}; UV–vis λ 618 (ε 115000 M^{-1} cm^{-1}) nm; Fluorescence (λ_{exc} 590 nm) λ_{em} 629 nm; ^1H NMR ($CDCl_3$) δ 1.37 (s, 6H), 2.54 (br t, $J = 7$ Hz, 4H), 2.88 (br t, $J = 7$ Hz, 4H), 3.22 (s, 1H), 7.23–7.45 (m, 8H), 7.65–7.69 (m, 2H), 8.81 (br d, $J = 7.8$ Hz, 2H); ^{13}C NMR ($CDCl_3$) δ 12.65, 20.75, 30.79, 78.80, 83.19, 123.03, 127.44, 128.18, 128.43, 128.73 (t, $J = 11$ Hz), 129.07, 129.57, 132.26, 132.96, 133.75, 135.95, 136.87, 138.67, 140.77, 150.98; ^{19}F NMR ($CDCl_3$) δ −134.5 (q, $J = 34$ Hz). HRMS Calcd for $C_{35}H_{27}BF_2N_2^+$ (M^+): 524.2230. Found (MALDI, matrix: DCTB): 524.22353.

Difluoro{3-methyl-2-[(3-methyl-4,5-dihydro-2*H*-benzo[*g*]indol-2-ylidene-*κN*)(4-{[4-({4-[(trimethylsilyl)ethynyl]phenyl}ethynyl)phenyl]ethynyl}phenyl)methyl]-4,5-dihydro-1*H*-benzo[*g*]indolato-*κN*}boron (37). Compounds **36** (139 mg, 0.265 mmol) and **29**[20a] (147 mg, 0.367 mol), [$Pd(PPh_3)_4$] (15 mg, 0.013 mmol), and CuI (2.5 mg, 0.013 mmL) were mixed in dry THF (7.5 mL), and the mixture was degassed by freeze–pump–thaw cycles. $Et(i\text{-}Pr)_2N$ (0.27 mL, 1.59 mmol) was added, and the dark blue mixture was stirred under Ar for 5 d. The mixture was filtered through Celite, and the solvent was evaporated. FC (SiO_2; CH_2Cl_2/cyclohexane 2/3) gave compound **37** (162.5 mg, 77%) as a dark copper-red solid. $R_f = 0.38$ (SiO_2; CH_2Cl_2/cyclohexane 2/3); mp > 300 °C (decomp); IR ν 2936, 2832, 2153, 1552, 1524, 1463, 1435, 1422, 1400, 1366, 1326, 1306, 1275, 1248, 1230, 1194, 1157, 1082, 1034, 1015, 965, 944, 863, 833, 768, 748, 721, 706, 668, 641 cm^{-1}; UV–vis λ 322 (ε 105000 M^{-1} cm^{-1}), 618 (ε 138000 M^{-1} cm^{-1}) nm; Fluorescence (λ_{exc} 590 nm) λ_{em} 629 nm; ^1H NMR ($CDCl_3$) δ 0.27 (s, 9H), 1.41 (s, 6H), 2.54 (br t, $J = 7$ Hz, 4H), 2.89 (br t, $J = 7$ Hz, 4H), 7.24–7.33 (m, 4H), 7.38–7.49 (m, 8H), 7.52–7.59 (m, 4H), 7.70–7.73 (m, 2H), 8.82 (br d, $J = 7.8$ Hz, 2H); ^{13}C NMR ($CDCl_3$) δ 0.28, 12.70, 20.77, 30.80, 90.67, 90.90, 91.05, 91.35, 96.72, 104.70, 122.95, 123.09, 123.35, 123.96, 127.45, 128.20, 128.46, 128.74 (t, $J = 11$ Hz), 129.15, 129.57, 131.53, 131.75, 132.06, 132.26, 132.24, 133.82, 135.98, 136.50, 138.86, 140.77, 150.97; ^{19}F NMR ($CDCl_3$) δ −134.5 (q, $J = 33.5$ Hz). HRMS Calcd for $C_{54}H_{43}BF_2N_2Si$ (M^+): 796.32566. Found (MALDI, matrix: DCTB): 796.3238.

(2-{[4-({4-[(4-Ethynylphenyl)ethynyl]phenyl}ethynyl)phenyl]-(3-methyl-4,5-dihydro-2*H*-benzo[*g*]indol-2-ylidene-*κN*)methyl}-

3-methyl-4,5-dihydro-1*H*-benzo[*g*]indolato-*κN*)(difluoro)boron (34). Compound **37** (155 mg, 0.195 mmol), *n*-Bu_4NF (0.235 mL, 0.235 mmol), and AcOH (0.03 mL) were allowed to react in THF (30 mL) according to General Procedure C. Crude FC (SiO_2; CH_2Cl_2), followed by trituration with $CHCl_3$ (5 mL) and THF (2 mL), gave compound **34** (138 mg, 97%) as a dark copper-red solid. The compound is poorly soluble in most common organic solvents. $R_f = 0.35$ (SiO_2; CH_2Cl_2/cyclohexane 1/1); mp > 300 °C (decomp); IR ν 3283, 2944, 2832, 1551, 1517, 1465, 1430, 1423, 1386, 1365, 1339, 1321, 1302, 1274, 1228, 1187, 1154, 1082, 1059, 1040, 1016, 963, 945, 904, 841, 833, 822, 775, 758, 751, 731, 715, 707, 646 cm^{-1}; UV–vis λ 320 (ε 77400 M^{-1} cm^{-1}), 571 (ε 21600 M^{-1} cm^{-1}), 618 (ε 103000 M^{-1} cm^{-1}) nm; Fluorescence (λ_{exc} 590 nm) λ_{em} 628 nm; ^{1}H NMR ($CDCl_3$) δ 1.41 (s, 6H), 2.54 (br t, $J = 7$ Hz, 4H), 2.89 (br t, $J = 7$ Hz, 4H), 3.19 (s, 1H), 7.24–7.33 (m, 4H), 7.39–7.45 (m, 4H), 7.49 (s, 4H), 7.52–7.59 (m, 4H), 7.70–7.73 (m, 2H), 8.82 (br d, $J = 7.8$ Hz, 2H); ^{13}C NMR (125 MHz, $CDCl_3$) δ 12.58, 20.70, 30.74, 91.17, 127.58, 128.30, 128.45, 128.60, 128.80, 128.89, 129.26, 129.30, 129.69, 131.74, 131.87, 131.91, 132.36, 132.39, 132.55, 132.57, 140.91, 140.93; ^{19}F NMR ($CDCl_3$) δ −134.5 (q, $J = 33.5$ Hz). HRMS Calcd for $C_{51}H_{35}BF_2N_2^+$ (M^+): 724.28613. Found (MALDI, matrix: DCTB): 724.2845.

{3-Ethyl-5-[(4-ethyl-3,5-dimethyl-2*H*-pyrrol-2-ylidene-*κN*)-(4-{[4-((17*s*,18*S*,19*r*,20*R*)-17,18,19,20-tetrahexyl-15^5,15^7(15^6*H*)-dioxo-2,4,6,8,10,12,14,16-octaoxa-15^5*H*-3,7,11(2,3)-triquinoxalina-15(2,3)-pyrrolo[3,4-*b*]pyrazina-1,5,9,13(1,2,4,5)-tetrabenzenapentacyclo[11.3.1.1^{1,5}.1^{5,9}.1^{9,13}]icosaphan-15^6-yl)-3,5-dimethylphenyl]ethynyl}phenyl)methyl]-2,4-dimethyl-1*H*-pyrrolato-*κN*)(difluoro)boron (38). Method A: Compounds **17** (30 mg, 0.019 mmol) and **28** (8.5 mg, 0.021 mmol), [$Pd(PPh_3)_4$] (1.2 mg, 0.001 mmol), and CuI (0.2 mg, 0.001 mmol) were mixed in dry THF (0.6 mL), and the mixture was degassed by freeze–pump–thaw cycles. Et(*i*-Pr)$_2$N (0.02 mL, 0.12 mmol) was added, and the bright red mixture degassed again and left to stir under Ar for 3 d. The solvent was evaporated, and FC (SiO_2; CH_2Cl_2/EtOAc gradient 0 → 2%), followed by GPC (CH_2Cl_2) afforded compound **38** (20 mg, 56%).

Method B: Compounds **18** (29.7 mg, 0.020 mmol) and **26** (11.2 mg, 0.022 mmol), [$Pd(PPh_3)_4$] (1.2 mg, 0.001 mmol), and CuI (0.2 mg, 0.001 mmol) were mixed in dry THF (0.8 mL), and the mixture was degassed by freeze–pump–thaw cycles. Et(*i*-Pr)$_2$N (0.02 mL, 0.12 mmol) was added and the bright red mixture degassed again and left to stir under Ar for 3 d. The mixture was evaporated to dryness, and FC (SiO_2; CH_2Cl_2/EtOAc gradient 1 → 2%), followed by GPC (CH_2Cl_2), yielded compound **38** (23.8 mg, 64%). Bright red solid. $R_f = 0.42$ (SiO_2; CH_2Cl_2/EtOAc, 1%); mp 270–290 °C (decomp); IR ν 2960, 2925, 2863, 1537, 1519, 1471, 1403, 1386, 1315, 1261, 1186, 1114, 1052, 1005, 974, 836, 819, 760, 705, 660 cm^{-1}; UV–vis λ 529 (ε 66800 M^{-1} cm^{-1}) nm; Fluorescence (λ_{exc} 490 nm) λ_{em} 542 nm; ^{1}H NMR ($CDCl_3$) δ 0.91–0.96 (m, 12H), 1.01 (t, $J = 7.5$ Hz, 6H), 1.07 (s, 3H), 1.32–1.52 (m, 38H), 2.20 (s, 3H), 2.22–2.38 (m, 12H), 2.56 (s, 6H), 5.52–5.69 (m, 4H), 7.21–7.39 (m, 9H), 7.46–7.51 (m, 5H), 7.69–7.72 (m, 2H), 7.76–7.82 (m, 2H), 7.85–7.93 (m, 4H), 8.20 (s, 2H), 8.22 (s, 2H); ^{13}C NMR ($CDCl_3$) δ 12.28, 12.91, 14.41, 14.97, 17.43, 17.90, 18.39, 22.99, 28.25, 29.68, 32.18, 32.62, 32.76, 32.84, 34.54, 118.71, 119.25, 123.51, 123.59, 123.78, 124.81, 127.63, 127.97, 128.79, 128.89, 129.02, 129.20, 129.40, 130.65, 131.39, 132.04, 132.42, 133.11, 135.60, 135.81, 135.89, 136.36, 136.70, 136.97, 137.54, 138.27, 139.19, 139.60, 139.67, 139.83, 141.50, 152.12, 152.41, 152.48, 152.57, 152.73, 152.87, 154.19, 158.75, 161.38; ^{19}F NMR ($CDCl_3$) δ −145.2 (q, $J = 32.5$ Hz). HRMS Calcd for $C_{115}H_{110}BFN_{11}O_{10}^+$ ($M^+ - F$): 1834.85087. Found (MALDI, matrix: DHB): 1834.8514.

Determination of the Activation Parameters for Kite1–Kite2 Switching of Cavitand 24. Fitting of NMR spectra was performed with the *g*NMR v3.6 for Macintosh program (Cherwell Scientific Publishing, Ltd., Oxford, UK). For the lineshape fitting of the kite1–kite2 equilibrium of cavitand **24**, enyne protons were used in a two-site exchange model. Determination of activation enthalpy and entropy was performed using the method described by Sandström:[31]

$$\log(k/T) = -\Delta H^{\neq}/aT + \Delta S^{\neq}/a + 10.319, \quad (1)$$

where k [Hz] is an exchange constant obtained from spectral fitting, T the temperature in Kelvin, and $a = 1.914 \times 10^{-2}$ for $\Delta H^{\neq}$ in kJ mol^{-1} and $\Delta S^{\neq}/a$ in kJ mol^{-1} K^{-1}. According to Eq. 1, a plot of $\log(k/T)$ vs $1/T$ (Eyring plot) has a slope of $(-\Delta H^{\neq}/a)$ and an intercept at $1/T = 0$ of $(\Delta S^{\neq}/a + 10.319)$.

Support by the Swiss National Science Foundation, via the National Research Program "Supramolecular Functional Materials" and the NCCR "Nanoscale Science" is gratefully acknowledged. We thank Dr. C. Thilgen (ETH) for help with the nomenclature.

References

1 a) Special issue on molecular machines: *Acc. Chem. Res.* **2001**, *34*, 410. b) *Molecular Switches*, ed. by B. L. Feringa, Wiley-VCH, Weinheim, Germany, **2001**. c) M. Irie, *Chem. Rev.* **2000**, *100*, 1685.

2 a) S. Kang, S. A. Vignon, H.-R. Tseng, J. F. Stoddart, *Chem. Eur. J.* **2004**, *10*, 2555. b) H.-R. Tseng, S. A. Vignon, J. F. Stoddart, *Angew. Chem., Int. Ed.* **2003**, *42*, 1491. c) J. W. Choi, A. H. Flood, D. W. Steuerman, S. Nygaard, A. B. Braunschweig, N. N. P. Moonen, B. W. Laursen, Y. Luo, E. DeIonno, A. J. Peters, J. O. Jeppesen, K. Xu, J. F. Stoddart, J. R. Heath, *Chem. Eur. J.* **2005**, *12*, 261.

3 G. Bottari, D. A. Leigh, E. M. Pérez, *J. Am. Chem. Soc.* **2003**, *125*, 13360.

4 a) M. C. Jimenez-Molero, C. Dietrich-Buchecker, J.-P. Sauvage, *Chem. Commun.* **2003**, 1613. b) M. C. Jimenez, C. Dietrich-Buchecker, J.-P. Sauvage, *Angew. Chem., Int. Ed.* **2000**, *39*, 3284.

5 a) M. Barboiu, G. Vaughan, N. Kyritsakas, J.-M. Lehn, *Chem. Eur. J.* **2003**, *9*, 763. b) M. Barboiu, J.-M. Lehn, *Proc. Natl. Acad. Sci.* **2002**, *99*, 5201.

6 M. Barboiu, L. Prodi, M. Montalti, N. Zaccheroni, N. Kyritsakas, J.-M. Lehn, *Chem. Eur. J.* **2004**, *10*, 2953.

7 a) T. Lougheed, V. Borisenko, T. Hennig, K. Rück-Braun, G. A. Woolley, *Org. Biomol. Chem.* **2004**, *2*, 2798. b) D. C. Burns, D. G. Flint, J. R. Kumita, H. J. Feldman, L. Serrano, Z. Zhang, O. S. Smart, G. A. Woolley, *Biochemistry* **2004**, *43*, 15329.

8 M. J. Pandya, E. Cerasoli, A. Joseph, R. G. Stoneman, E. Waite, D. N. Woolfson, *J. Am. Chem. Soc.* **2004**, *126*, 17016.

9 For a preliminary communication of parts of this work, see: V. A. Azov, A. Schlegel, F. Diederich, *Angew. Chem., Int. Ed.* **2005**, *44*, 4635.

10 a) J. R. Moran, S. Karbach, D. J. Cram, *J. Am. Chem. Soc.* **1982**, *104*, 5826. b) J. R. Moran, J. L. Ericson, E. Dalcanale, J. A. Bryant, C. B. Knobler, D. J. Cram, *J. Am. Chem. Soc.* **1991**, *113*, 5707. c) D. J. Cram, H.-J. Choi, J. A. Bryant, C. B. Knobler,

J. Am. Chem. Soc. **1992**, *114*, 7748. d) D. J. Cram, J. M. Cram, *Container Molecules and Their Guests*, Royal Society of Chemistry, Cambridge, **1994**, pp. 107–130.

11 a) F. Hof, S. L. Craig, C. Nuckolls, J. Rebek, Jr., *Angew. Chem., Int. Ed.* **2002**, *41*, 1488. b) J. Rebek, Jr., *Angew. Chem., Int. Ed.* **2005**, *44*, 2068. c) P. Soncini, S. Bonsignore, E. Dalcanale, F. Ugozzoli, *J. Org. Chem.* **1992**, *57*, 4608.

12 P. J. Skinner, A. G. Cheetham, A. Beeby, V. Gramlich, F. Diederich, *Helv. Chim. Acta* **2001**, *84*, 2146.

13 M. Frei, F. Marotti, F. Diederich, *Chem. Commun.* **2004**, 1362.

14 a) V. A. Azov, B. Jaun, F. Diederich, *Helv. Chim. Acta* **2004**, *87*, 449. b) P. Roncucci, L. Pirondini, G. Paderni, C. Massera, E. Dalcanale, V. A. Azov, F. Diederich, *Chem. Eur. J.* **2006**, *12*, 4775.

15 a) V. A. Azov, F. Diederich, Y. Lill, B. Hecht, *Helv. Chim. Acta* **2003**, *86*, 2149. b) V. A. Azov, P. J. Skinner, Y. Yamakoshi, P. Seiler, V. Gramlich, F. Diederich, *Helv. Chim. Acta* **2003**, *86*, 3648.

16 a) T. Förster, *Ann. Phys.* **1948**, *2*, 55. b) P. R. Selvin, *Methods Enzymol.* **1995**, *246*, 300.

17 M. Vincenti, E. Dalcanale, P. Soncini, G. Guglielmetti, *J. Am. Chem. Soc.* **1990**, *112*, 445.

18 a) A. R. Renslo, F. C. Tucci, D. M. Rudkevich, J. Rebek, Jr., *J. Am. Chem. Soc.* **2000**, *122*, 4573. b) F. C. Tucci, A. R. Renslo, D. M. Rudkevich, J. Rebek, Jr., *Angew. Chem., Int. Ed.* **2000**, *39*, 1076. c) U. Lücking, F. C. Tucci, D. M. Rudkevich, J. Rebek, Jr., *J. Am. Chem. Soc.* **2000**, *122*, 8880. d) S. D. Starnes, D. M. Rudkevich, J. Rebek, Jr., *J. Am. Chem. Soc.* **2001**, *123*, 4659. e) U. Lücking, J. Chen, D. M. Rudkevich, J. Rebek, Jr., *J. Am. Chem. Soc.* **2001**, *123*, 9929.

19 S.-W. Kang, P. P. Castro, G. Zhao, J. E. Nunez, C. E. Godinez, L. M. Gutierrez-Tunstad, *J. Org. Chem.* **2006**, *71*, 1240.

20 a) O. Lavastre, L. Ollivier, P. H. Dixneuf, S. Sibandhit, *Tetrahedron* **1996**, *52*, 5495. b) I. Aujard, J. P. Baltaze, J. B. Baudin, E. Cogne, F. Ferrage, L. Jullien, E. Perez, V. Prevost, L. M. Qian, O. Ruel, *J. Am. Chem. Soc.* **2001**, *123*, 8177.

21 J. Olsen, P. Seiler, B. Wagner, H. Fischer, T. Tschopp, U. Obst-Sander, D. W. Banner, M. Kansy, K. Müller, F. Diederich, *Org. Biomol. Chem.* **2004**, *2*, 1339.

22 Spartan 04 for Windows, Wavefunction Inc., 18401 Von Karman Ave., Irvine, CA 92612, U.S.A.

23 H. B. Bürgi, J. D. Dunitz, *Acc. Chem. Res.* **1983**, *16*, 153.

24 a) K. Sonogashira, T. Yatake, Y. Tohda, S. Takahashi, N. Hagihara, *J. Chem. Soc., Chem. Commun.* **1977**, 291. b) K. Sonogashira, in *Metal-Catalyzed Cross-Coupling Reactions*, ed. by F. Diederich, P. J. Stang, Wiley-VCH, Weinheim, **1998**, pp. 203–229. c) J. A. Marsden, M. M. Haley, in *Metal-Catalyzed Cross-Coupling Reactions*, 2nd ed., ed. by A. de Meijere, F. Diederich, Wiley-VCH, Weinheim, **2004**, Vol. 1, pp. 317–394.

25 P. P. Castro, G. Zhao, G. A. Masangkay, C. Hernandez, L. M. Gutierrez-Tunstad, *Org. Lett.* **2004**, *6*, 333.

26 a) J. Karolin, L. B.-Å. Johansson, L. Strandberg, T. Ny, *J. Am. Chem. Soc.* **1994**, *116*, 7801. b) A. Burghart, H. Kim, M. B. Welch, L. H. Thoresen, J. Reibenspies, K. Burgess, F. Bergström, L. B.-Å. Johansson, *J. Org. Chem.* **1999**, *64*, 7813. c) J. Chen, A. Burghart, A. Derecskei-Kovacs, K. Burgess, *J. Org. Chem.* **2000**, *65*, 2900. d) A. Burghart, L. H. Thoresen, J. Chen, K. Burgess, F. Bergström, L. B.-Å. Johansson, *Chem. Commun.* **2000**, 2203. e) G. Ulrich, R. Ziessel, *J. Org. Chem.* **2004**, *69*, 2070.

27 H. Ihm, J.-S. Ahn, M. S. Lah, Y. H. Ko, K. Paek, *Org. Lett.* **2004**, *6*, 3893.

28 a) S. Weiss, *Science* **1999**, *283*, 1676. b) B. Hecht, B. Sick, U. P. Wild, V. Deckert, R. Zenobi, O. J. F. Martin, D. W. Pohl, *J. Chem. Phys.* **2000**, *112*, 7761.

29 V. R. Holland, B. M. Roberts, B. C. Saunders, *Tetrahedron* **1969**, *25*, 2291.

30 K.-S. Jeong, Y. L. Cho, S.-Y. Chang, T.-Y. Park, J. U. Song, *J. Org. Chem.* **1999**, *64*, 9459.

31 J. Sandström, *Dynamic NMR Spectroscopy*, Academic Press, London, **1982**, pp. 93–123.